Huchon, P., Taylor, B., and Klaus, A. (Eds.)
Proceedings of the Ocean Drilling Program, Scientific Results Volume 180

Active Continental Extension in the Western Woodlark Basin: A Synthesis of Leg 180 Results[1]

Brian Taylor[2] and Philippe Huchon[3]

ABSTRACT

During Leg 180 we collected core and borehole data from a transect of sites drilled in a region of rapid extension (Moresby rift and Moresby Seamount) and its less extended northern margin (Woodlark Rise) that is at the point of continental breakup adjacent to the Woodlark spreading center. Postcruise analysis of these data and parallel investigations provide new insights into the nature of the continental crust being rifted, the style of synrift (and prerift) sedimentation, the mechanisms of rifting (including shallow-angle normal faulting and lower crustal flow), and the extent of the deep biosphere.

The upper crust of the Papuan region (onshore and offshore) is composed of a variety of basement types (dominantly ophiolitic normal mid-ocean-ridge basalt [N-MORB] and enriched mid-ocean-ridge basalt [E-MORB], but also island arc rocks) and ages (late Maastrichtian, Paleocene, and middle Eocene). The Site 1117 gabbro crystallized in the late Maastrichtian (66 Ma) and, together with the thick E-MORB dolerite sill complex at Sites 1109 and 1118 and probably the metadolerite at Site 1114, cooled into the Paleocene (59–54 Ma), and all were partially altered through the early Oligocene. Archean continental components exist in the lower crust.

This amalgam of oceanic, arc, and continental basement terranes was the site of early Miocene to Holocene arc magmatism related to southward subduction at the Trobriand Trough. A thick forearc basin developed in the Miocene, which filled to sea level in the late Miocene from paleowater depths >500 m. Volcaniclastic turbidites indicate source ter-

[1]Taylor, B., and Huchon, P., 2002. Active continental extension in the western Woodlark Basin: a synthesis of Leg 180 results. *In* Huchon, P., Taylor, B., and Klaus, A. (Eds.), *Proc. ODP, Sci. Results,* 180, 1–36 [Online]. Available from World Wide Web: <http://www-odp.tamu.edu/publications/180_SR/VOLUME/SYNTH/SYNTH.PDF>. [Cited YYYY-MM-DD]
[2]Department of Geology and Geophysics, SOEST, University of Hawaii, 1680 East-West Road, Honolulu HI 96822-2285, USA. **taylorb@hawaii.edu**
[3]Géosciences Azur, Observatoire océanologique de Villefranche s/mer, Université Pierre et Marie Curie, BP 48, 06235 Villefranche s/mer, France.

Initial receipt: 18 July 2001
Acceptance: 7 January 2002
Web publication: 3 May 2002
Ms 180SR-150

ranes of calc-alkaline extrusives, dominantly basaltic, with lesser rhyolitic and, rarely, alkalic rocks.

A regional unconformity at 8.4 Ma marks the onset of rifting and provides a paleo–sea level surface for tracking the subsequent subsidence of the northern margin sites from paralic to shelf to the present bathyal water depths. The northward Miocene drainage was reversed as the margin thinned and subsided southward toward the active rifts. Moresby Seamount was not a topographic high in the late Miocene. It was part of a wide graben system that included the basin to the south as well as what is now Moresby rift. All the master faults that currently bound these basins were formed early in the rift history, and at least one of them initiated at shallow dips.

Clastics, largely deposited by turbidity currents with higher energy environments in the rift basins than on the margins, were derived from calc-alkaline volcanics plus pelitic metamorphic rocks and lesser ultramafic rocks. The turbidite bed thicknesses fit a power-law model, most likely controlled by earthquakes. High-K volcanic ash layers and muds rich in tephra intersected at Sites 1109 and 1115 at <2.3 Ma record explosive eruptions from rhyolitic volcanoes of the D'Entrecasteaux Islands, both peralkaline (Dawson Strait) and calc-alkaline (Moresby Strait).

Movement in the Pleistocene on the normal faults that bound Moresby Seamount uplifted the footwall seamount, lowered the hanging-wall rift basins, and substantially changed the paleogeography and depositional pathways. Terrigenous sediments ceased to onlap the northern margin during the Pleistocene (~1.2 Ma), and since that time sedimentation in Moresby rift, other than pelagics, has been limited to talus derived from fault scarps plus sediments eroded from the northern margin.

Within the ~100-m-thick Moresby normal fault zone at Site 1117 (gouge, mylonite, breccia, and undeformed quartz gabbro), mylonites and calcite twins indicate depths and temperatures greater than those indicated by other lines of evidence. For example, the gabbros were not thermally reset from their 66-Ma ages and must have stayed at shallow and cool levels in the crust. Dynamic shear heating may explain this paradox.

The Moresby normal fault dips ~30°N, consistent with the frictional properties expected for mature faults with well-developed gouge zones. The propensity for failure at the shallow dips observed is overdetermined; there is evidence for both

1. Fault weakening as a consequence of (a) high slip rates and (b) talc-chlorite-serpentine gouge mineralogy and
2. Enhanced hydrothermal fluid migration within the permeable, porous, and anisotropic fault zone at greater than hydrostatic fluid pressures.

Such shallow-angle normal faults may be a common feature of strain localization in the transition from rifting to spreading.

The up to 3 km of subsidence of the cold (30 mW/m^2) northern margin, with little attendant brittle deformation, requires substantial crustal thinning by lower crustal flow. This ductile extension is demonstrably not activated by temperature but presumably by fluids and occurs synrift, not just postbreakup.

Organic carbon and pyrolysis gas chromatographic data indicate that there is no significant source rock potential at Site 1108, although suffi-

cient organic matter (0.6 ± 0.5 wt%) is present for microbial processes to generate the limited gas present within the recovered cores. The hydrocarbons encountered appear to be indigenous and not a migrated product or contaminant, suggesting that Site 1108 can be revisited safely in order to penetrate and characterize the in situ properties of the Moresby normal fault at depth.

Culturable anaerobic bacteria and realistic rates of anaerobic bacterial activity (sulfate reduction, methanogenesis, and thymidine incorporation) are present in the deepest samples from the subseafloor biosphere analyzed to date for microbial populations (842 meters below seafloor [mbsf]; Site 1118) and activities (800 mbsf; Site 1115).

INTRODUCTION

The rifting and breakup of continental lithosphere has produced conjugate passive margins with a rich diversity of structural, magmatic, and sedimentary architectures. Yet only a handful of modern examples exist where these processes are active and so may be examined in situ. During Ocean Drilling Program (ODP) Leg 180 we investigated one of these examples in the western Woodlark Basin of Papua New Guinea (Fig. F1). This is an area of low- and high-angle normal faulting, metamorphic core complex formation, and seafloor spreading that has been propagating westward into rifting lithosphere since 6 Ma (e.g., see review in Taylor, 1999). The Papuan continent being rifted is a young orogen with inherent complexities such as ophiolite emplacement in the Paleogene and Neogene arc magmatism.

We summarize the results of studies associated with the transect of holes drilled during Leg 180 along ~151°35′E from 9°11′ to 9°52′S (Fig. F2). The drilling transect was focused on the center of active deformation (Moresby rift) in front of the spreading tip and on the adjacent rift margins: Sites 1114 and 1116 on Moresby Seamount to the south and Sites 1109, 1115, and 1118 on the Woodlark Rise to the north. We had planned a cased reentry hole to intersect at ~900 meters below sea level (mbsl) the ~27°N-dipping Moresby fault in order to characterize the in situ properties of an active low-angle normal fault. Shipboard concerns about the presence of trace hydrocarbons encountered at Site 1108 and impenetrable drilling conditions in talus aprons encountered at Sites 1110–1113 thwarted those plans. The Moresby fault was penetrated, but only at Site 1117, where it cropped out at 1163 mbsl.

We review new dating, geochemistry, and petrofabric studies that permit an evaluation of the origin and deformation history of the basement. Analyses of the cores and logs, in the context of a regional grid of seismic profiles, provides a high-resolution record of margin subsidence, sedimentation, and paleoenvironment. Detailed investigations of the core physical properties, structures, and pore fluids, together with log interpretation, have produced an understanding of the postdepositional changes, from diagenesis to deformation.

The results from Leg 180 document the upper crustal processes occurring in this region of continental rifting and breakup. Together with estimates of strain rate, thermal regime, and crustal structure, they also have implications for lower crustal flow and the mechanisms of crustal thinning. After some discussion of the regional context, our synthesis below proceeds from the basement to the depositional history, diagenesis-geochemistry-microbiology, and then to the deformation.

F1. Major features of the Woodlark Basin region, p. 27.

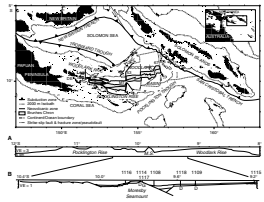

F2. Topography and bathymetry of the Leg 180 drilling transect, p. 28.

Each section is a mini-synthesis, and therefore we do not have a separate conclusion section.

REGIONAL GEOLOGY AND TECTONICS OF PAPUA

The region around the sites of Leg 180 drilling includes the Papuan Peninsula, D'Entrecasteaux Islands, and the conjugate rifted margins and islands of the Woodlark and Pocklington Rises (Fig. F3). As reviewed in Davies et al. (1984) and Taylor (1999), the tectonic history of interest begins in the Late Cretaceous with a passive margin and ocean bordering northeast Australia. Northward subduction within the oceanic lithosphere developed an island arc and pulled continental fragments, including the Papuan Plateau, from Australia by opening the Coral Sea Basin (62–52 Ma) (Weissel and Watts, 1979; Rogerson et al., 1993). Former Australian margin sediments (now Owen Stanley Metamorphics) were accreted at the trench until the Papuan Plateau was partially subducted and an arc-continent collision ensued (Davies and Jaques, 1984). This Paleogene orogeny formed the core of the paleo-Papuan Peninsula, much of which today is 1–3 km above sea level and is underlain by a crust 30–45 km thick (Ferris et al., 2000).

Southward (reversed direction) subduction along the Trobriand Trough produced arc magmatism from the early Miocene (possibly late Oligocene) through the Holocene (Davies and Smith, 1971; Davies et al., 1984; Hegner and Smith, 1992; Stolz et al., 1993). The modern volcanic front extends from Mt. Lamington (which erupted in 1951) through Mt. Victory to Fergusson Island and in the Pliocene continued to the Amphlett Islands and Egum Atoll (4.4- to 3.5- and 2.9-Ma andesite, respectively) (Smith and Milsom, 1984). Numerous Miocene–Holocene andesitic and lesser shoshonitic volcanic centers occur behind the volcanic front (Fig. F3). Trenchward, there is a forearc basin with depocenters up to 5–7 km thick bounded by an outer forearc basement high, capped by the Lusancay-Trobriand-Woodlark Islands (Tjhin, 1976; Pinchin and Bembrick, 1985; Francis et al., 1987).

Metamorphic core complexes developed along (D'Entrecasteaux Islands) or just behind (Misima, Suckling-Dayman massif, and Emo metamorphics) the volcanic front in the latest Miocene to Holocene (Davies, 1980; Davies and Warren, 1988, 1992; Hill et al., 1992, 1995; Baldwin et al., 1993; Hill and Baldwin, 1993; Lister and Baldwin, 1993; Hill, 1994; Martinez et al., 2001). Core complex formation accompanied continental rifting, peralkaline rhyolite volcanism (Smith, 1976), and westward propagation of seafloor spreading since at least 6 Ma that formed the oceanic Woodlark Basin (Weissel et al., 1982; Taylor and Exon, 1987; Taylor et al., 1995, 1999). West of 153°E, spreading split the formerly contiguous Woodlark and Pocklington Rises approximately along the volcanic line, producing inherently asymmetric conjugate passive margins, with a Neogene forearc to the north and a Paleogene collision complex to the south. East of 153°E, the Neogene volcanic arc terminates and the boundary between the Woodlark Rise and the Solomon Sea is a transform margin (Figs. F1, F3). Thus, the (eastern) Woodlark Basin, where spreading initiated, did not originate as a back-arc basin (Weissel et al., 1982).

F3. Simplified regional geology, p. 29.

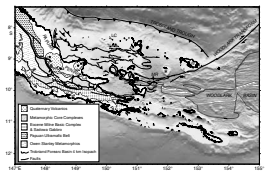

BASEMENT AGE AND COMPOSITION

Drilling at four Leg 180 sites penetrated basement (Fig. F1) and recovered a suite of dolerite (Sites 1109, 1114, and 1118) and gabbro (Site 1117) plus basalt in conglomerates (also at Site 1115). Metadolerites were also recovered as pebbles in talus at Sites 1110–1112. As the contacts with the basement were either unconformable (Sites 1109 and 1118) or faulted (Sites 1114 and 1117), the age and nature of the intrusives were uncertain; they could be related to the Papuan ophiolite, Miocene forearc basin, or late Miocene rifting (Shipboard Scientific Party, 1999).

Ion microprobe analyses of zircons in the Site 1117 gabbro gave a $^{238}U/^{206}Pb$ age of 66.4 ± 1.5 Ma (**Monteleone et al.,** this volume), whereas $^{40}Ar/^{39}Ar$ plagioclase apparent ages of basement samples from Sites 1109, 1117, and 1118 varied considerably with the extent of sample alteration (**Monteleone et al.; Brooks and Tegner,** both this volume). Some of the least-altered dolerites yielded $^{40}Ar/^{39}Ar$ plagioclase isochron ages of 58.9 ± 5.8 and 54 ± 1 Ma and plateau ages of 58.2 ± 1.0 and 55.6 ± 0.3 Ma (**Monteleone et al.; Brooks and Tegner,** both this volume). Variable alteration and associated Ar loss resulted in a suite of younger plagioclase apparent ages from 54 to 31 Ma.

Monteleone et al. (this volume) infer from these dates that the gabbro crystallized in the late Maastrichtian and, together with the dolerites, cooled into the Paleocene and was partially altered through the early Oligocene. They were not thermally reset by subsequent rifting events and so must have remained at shallow and cool (<250°C) levels in the crust (**Monteleone et al.,** this volume).

Brooks and Tegner (this volume) conducted inductively coupled plasma–mass spectrometer (ICP-MS) analyses of dolerites from Sites 1109 and 1118, as well as of Papuan Ultramafic Belt (PUB) (Jaques and Chappell, 1980) and Woodlark Island (Luluai volcanics) (Ashley and Flood, 1981) basalts. From the conservative trace elements least mobile during alteration, they conclude that the dolerites from Sites 1109 and 1118 consist of material derived by partial melting of enriched mantle. The dolerites are geochemically similar to the Woodlark Island basement (and Ontong Java Plateau) but are unlike the basalts of the PUB, which came from a source similar to that of normal mid-ocean-ridge basalt (N-MORB).

The initial interpretation of multichannel seismic (MCS) data in the vicinity of Sites 1118, 1109, and 1115 needs correcting in light of the new dates of basement. The Shipboard Scientific Party (1999) inferred that the well-layered reflectors dipping ~10°N beneath the late Miocene–Quaternary sediments on this part of the Woodlark Rise represented Miocene forearc basin sediments similar to those imaged and drilled north of the D'Entrecasteaux Islands (Tjhin, 1976; Francis et al., 1987). Although such sediments were intersected at Site 1115, reinterpretation of the regional grid of MCS and gravity data (Goodliffe et al., 1999) shows that Site 1115 occurs near the eastern edge of the forearc basin (Fig. F3). Less than 500 m of Miocene sediments occurs beneath Site 1115 (**Goodliffe et al.,** this volume), whereas the forearc basin is nearly 5 km thick only 15 km farther west (Fang, 2000).

The implication is that the >2.5 s two-way traveltime–thick prerift section of subparallel reflectors between Sites 1109 and 1115 represents >5 km of basement. Given the reflector geometry and the enriched mid-ocean-ridge basalt (E-MORB) character of the dolerites at Sites 1109

and 1118, this is apparently an extensive sill complex, possibly capped by basalts updip to the north of Site 1109. The alternative interpretation, that Sites 1109 and 1118 (and Site 1114) happened to intersect dikes within an otherwise thick lava sequence, is not supported by the lesser proportion of basalt vs. dolerite pebbles in the conglomerates derived from the erosion of basement. Although it is possible that the sequence has been thickened by thrust repetition, the simplest interpretation is that a thick igneous province was regionally tilted up on its southern edge, probably during the Paleogene orogeny, and subsequently extensively eroded. The presence of gabbro at ~1200 mbsl at Site 1117 in the same structural block of Moresby Seamount as dolerite at ~700 mbsl at Site 1114 is consistent with this interpretation.

It is instructive to compare what is now known about the ages and composition of basement in the Papuan region onshore and offshore. The PUB ocean tholeiites-gabbros-hartzburgites locally have a cover of Maastrichtian micrites (Davies, 1980). This age is correlative with the zircon age of crystallization for the Site 1117 gabbro. In other areas the foraminifer-bearing micrites overlying the PUB basalts are late Paleocene (P4 = 59–56 Ma) (Rogerson et al., 1993) in age. Other Paleocene ages include the cooling ages from Leg 180 dolerites and gabbros, as well as unpublished $^{40}Ar/^{39}Ar$ hornblende ages from PUB pegmatitic gabbros of 55.5 and 58.4 Ma (R. Duncan, pers. comm., 2001). K/Ar and $^{40}Ar/^{39}Ar$ hornblende ages of 66–56 Ma from granulites at the sole of the PUB in the Musa-Kumusi divide have been interpreted to date the PUB emplacement (Lus et al., 1998). Middle Eocene stratigraphic ages suggest that the large province of ocean tholeiites covering the southern part of the Papuan Peninsula (Milne Basic Complex and Sadowa Gabbro) (Smith, 1982) are younger than the PUB. The stratigraphically pre–late Oligocene Luluai volcanics on Woodlark Island have been considered to be equivalent to the Milne Basic Complex, but there are no radiometric ages to support this interpretation (Ashley and Flood, 1981; Davies et al., 1984).

Volcanics of island arc affinity also form part of the regional basement. Tholeiitic andesites and boninitic lavas from the Dabi Volcanics on Cape Vogel have $^{40}Ar/^{39}Ar$ total fusion and plateau ages of 58.9 ± 1 Ma, as well as 53.7 ± 1 Ma (Walker and McDougall, 1982). The Lokanu volcanics, intersected at the base of the Nubiam 1 well, are late Paleocene (Francis et al., 1987). Tonalite-diorite-dacite intrusions through the PUB are K/Ar dated at 57–47 Ma (Rogerson et al., 1993).

Thus, the upper crust of the Papuan Peninsula, D'Entrecasteaux Islands, and offshore regions of the Woodlark and Pocklington Rises is composed of a variety of basement types (dominantly ophiolitic N-MORB and E-MORB, but also arc tholeiites/boninites and dacites/tonalites) and ages (late Maastrichtian, Paleocene, and middle Eocene). The relations between many of its component parts remain unknown in detail. Furthermore, Archean zircons in Pliocene–Pleistocene conglomerates sourced from core complexes on Goodenough Island attest to the presence of Archean continental components in the lower crust (Baldwin and Ireland, 1995). These may derive from subducted parts of Australian continental fragments such as the Papuan Plateau.

This amalgam of oceanic, arc, and continental basement terranes superimposed by Neogene arc magmatism controls the rheology of the orogenic continent that is rifted in the late Miocene–Holocene. For example, Martinez et al. (2001) show that the prevalence of upper crustal ophiolites creates a density inversion capable of driving vertical extru-

sion of ductile lower crust in metamorphic core complexes such as that occurring in the D'Entrecasteaux Islands.

MIOCENE TROBRIAND FOREARC BASIN

Southward subduction along the Trobriand Trough produced arc magmatism in Papua since at least the early Miocene (Davies and Smith, 1971; Davies et al., 1984). During the early and middle Miocene, the Trobriand forearc was extensional and a forearc basin developed that filled with sediments up to 5–7 km thick (Tjhin, 1976; Pinchin and Bembrick, 1985; Francis et al., 1987). The basin was inverted in the west, and the outer forearc high was uplifted in the middle–late Miocene. Multiple reverse thrusts occur in the west, but the basin is more open north of the D'Entrecasteaux Islands where the depocenter shifted southward as the outer forearc was up-tilted (Tjhin, 1976; Pinchin and Bembrick, 1985; Francis et al., 1987). Farther east, from ~151°E to the Leg 180 drilling transect, the middle–late Miocene sediments prograded from the emergent Papuan Peninsula northward across the forearc to a depocenter just south of the outer forearc high (Davies et al., 1984; Taylor, 1999; Fang, 2000). The forearc basin filled to sea level in the late Miocene.

This Miocene forearc basin history is amply documented west of 151°E by commercial wells (Goodenough 1 and Nubiam 1) and seismic surveys (Tjhin, 1976; Pinchin and Bembrick, 1985; Francis et al., 1987). Of note, the early Miocene (and late Oligocene?) Iauga volcanics (tuffs and tuffaceous conglomerates) at the base of the Goodenough 1 well attest to the early Trobriand arc volcanism (Fig. **F4**). The middle Miocene was a time of deepwater deposition of (silty) shales with tuffaceous interbeds that in the late Miocene shoaled upward during deposition of the thick Nubiam shale (Fig. **F5**). Within the regional grid of seismic profiles tied to the two wells, horizon "A" marks an important late Miocene unconformity (or correlative conformity near the basin depocenter at Goodenough 1 well) (Tjhin, 1976; Pinchin and Bembrick, 1985; Francis et al., 1987) beneath the pro-delta Ruaba unit.

More recent seismic surveys (Mutter et al., 1996; Goodliffe et al., 1999; Fang, 2000) and Leg 180 drilling at Site 1115 now confirm and extend this history to the eastern end of the forearc basin. A rapidly deposited (>375 m/m.y.) sequence of middle Miocene (~14–13 Ma) volcaniclastic clays, silts, and sands was recovered at Site 1115 beneath a late Miocene unconformity (correlative to horizon "A") (Figs. **F6, F7**) (Shipboard Scientific Party, 1999; Lackschewitz et al., 2001; **Takahashi et al.,** this volume). Paleowater depths, initially >500 m, shoal upward, accompanied by an increasing component of redeposited shallow-water carbonates. Lithic fragments and geochemical analyses of the volcaniclastics indicate source terranes of calc-alkaline extrusives, dominantly basic with lesser rhyolitic and rare alkalic (**Sharp and Robertson; Robertson and Sharp; Cortesogno et al.,** all this volume). Two rhyolitic clasts (in Pleistocene talus from Sites 1110 and 1111) gave $^{238}U/^{206}Pb$ zircon ages of 15.7 ± 0.4 Ma and provide further evidence for middle Miocene Trobriand arc volcanism (**Monteleone et al.,** this volume). Sporadic appearances of high Cr and Ni contents in fine-grained sediments at Leg 180 sites suggest that ultramafic source rocks were exposed/weathering since at least the middle Miocene (**Robertson and Sharp,** this volume).

F4. Well correlation diagram, p. 30.

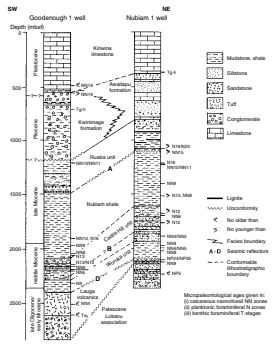

F5. Sedimentation curves at the Goodenough 1 and Nubiam 1 wells, p. 31.

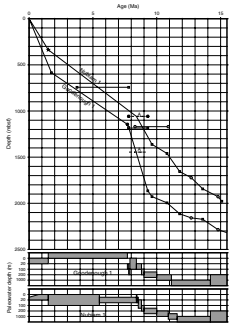

F6. Lithostratigraphy and correlation of Leg 180 sites, p. 32.

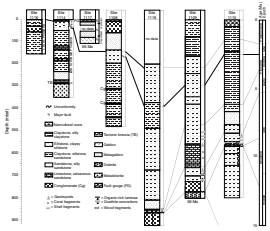

F7. Sedimentation curves and paleobathymetry ranges, p. 33.

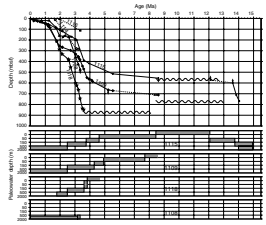

Although the record is clear, the cause of the late Miocene forearc emergence is uncertain. The compression in the west may be related to early phases of the collision of the Huon-Finisterre forearc with the Trobriand forearc, resulting from the progressive closure of the Solomon Sea by doubly vergent subduction (Fig. F1) (Jaques and Robinson, 1977; Cooper and Taylor, 1987; Pegler et al., 1995). However, the extent of the late Miocene unconformity around the Trobriand forearc basin begs a more regional cause. It may be subduction related and/or it may be related to the onset of rifting. But it certainly reflects increased sediment supply from increasingly emergent margins (Smith and Davies, 1976), in part the result of the largest fall in global sea level during the Tertiary (~225 m between 15 and 10 Ma) (Haq et al., 1988).

The age of the unconformity surface is best defined by the correlative conformity at the Goodenough 1 well. Our reexamination of the reported biostratigraphy there shows that horizon "A" (at the base of the Ruaba unit at 1445 meters below seafloor [mbsf]) is located between the first and last occurrences of *Minylitha convallis* (i.e., between 9.3 and 7.8 Ma) (Berggren et al., 1995, p. 190) at 1865 and 1180 mbsf. Direct interpolation (equivalent to assuming a constant sedimentation rate for this interval of 457 m/m.y.) places horizon "A" at 8.4 Ma (Fig. F5). This result fits well with the age constraints from the other drill holes, namely that there are sediments beneath the unconformity at the Nubiam 1 well that are younger than 9.3 and older than 8.3 Ma and that sediments above it at Site 1115 are younger than 8.6 and older than 5.54 Ma (Figs. F5, F6, F7).

The extent of the late Miocene erosion varies, from none at Goodenough 1 well near the contemporary basin depocenter to 4–5 m.y. of missing section at Site 1115 near the eastern basin edge. That the amount of actual uplift of much of the eastern forearc basin may have been quite small (<50 m) is attested by seismic reflection profiles that show the preservation of the topsets of prograding clinoforms immediately beneath the unconformity (Taylor, 1999; Fang, 2000). Furthermore, the angular change in bedding orientation across the unconformity at Site 1115 is small, from dipping 5°–10° to the northwest (toward the forearc basin depocenter) to horizontal (**Célérier et al.,** this volume). This stratal geometry also confirms that the 8.4-Ma unconformity surface approximates paleo–sea level, which provides an important horizon for tracking subsequent vertical tectonics.

LATE MIOCENE ONSET OF RIFTING: TIMING AND INITIAL SUBSIDENCE

The timing of, and vertical motions associated with, the onset of rifting are important parameters for models of continental rifting processes. In many areas, however, including the North Atlantic, these critical aspects are only broadly constrained (e.g., Wilson et al., 2001). It is important, therefore, to critically appraise the data bearing on this issue in the case of the western Woodlark Basin. Some framework information comes from the opening history of the Woodlark Basin, which we know had begun spreading by 6 Ma in the east and has since been propagating westward into rifting lithosphere (Taylor et al., 1999). Additional data comes from the metamorphic core complex on Misima Island, where high-grade metamorphic rocks occur beneath a low-angle (23°N) normal fault and low-grade cover rocks. Preliminary thermo-

chronologic data indicate granite intrusion and deformation occurred at ~8 Ma, with subsequent hydrothermal alteration and ore mineralization from 4.0 to 3.2 Ma (Baldwin et al., 2000).

Ascribing the 8.4-Ma unconformity to rift onset is consistent with existing information, but it is not a unique interpretation of the margin stratigraphy and vertical motions, given the possible subduction and known eustatic effects discussed above. Indeed, the late Miocene subsidence and depositional history data from sites drilled on the Woodlark Rise alone are equivocal on this issue. Nevertheless, seismic horizons dated at these sites can be correlated into the Moresby rift and confirm that rift faulting began by ~8 Ma (see below).

A distinctive paleogeography and depositional facies characterizes the Trobriand forearc and the Woodlark Rise in the late Miocene above the 8.4-Ma unconformity. Everywhere in the forearc was either shallow-water (<50 m) or low-relief islands (such as the ~300-m basement high drilled at Site 1118, where lateritic paleosols are present in the interstices between dolerite and basalt clasts in a >50-m-thick conglomerate). The stratigraphic record at Sites 1109 and 1115 and Goodenough 1 and Nubiam 1 wells reflects a paralic region of islands, lagoons, algal reefs, swamps, and deltas fed by rivers draining upland to the south (Shipboard Scientific Party, 1999; Francis et al., 1987; Robertson et al., 2001). Sediment isopachs show that Site 1109 was drilled near the axis and Site 1118 is on the flank of one such paleochannel (Goodliffe et al., 1999). Conglomerates of basalt (at Site 1115) and dolerite and basalt (at Site 1109) that immediately overlie the unconformity were deposited in a fluvial to swampy setting (Shipboard Scientific Party, 1999). The overlying lagoonal facies is brackish at Site 1109 (with shell, plant, and wood fragments common) to initially relatively enclosed and then more open marine at Site 1115 (with abundant shell fragments) (Shipboard Scientific Party, 1999). Chemically distinctive claystones and siltstones (with higher Ti and Fe_2O_3 and lower K than calc-alkaline-sourced sediments) are compatible with derivation from an exposed and tropically weathered basic igneous basement (**Robertson and Sharp,** this volume).

What caused the initial accommodation space above the 8.4-Ma unconformity? One factor was the net ~120-m sea level rise between 8 and 5 Ma (Haq et al., 1988). Another was possibly residual thermal subsidence following earlier forearc basin extension. Seismic profiles show that lensoid stratal packages that onlap the forearc basin edges persist between Sites 1109 and 1115 and farther west until ~3.2 Ma (Fig. **F8**) (**Goodliffe et al.,** this volume; Fang, 2000). This sag phase of shelf deposition can be modeled as thermal subsidence from the previous extension, and thus is not a reliable indicator of contemporary rifting.

The telltale sign of the onset of rifting is not to be found on the northern margin (the Woodlark Rise) but in the early graben such as Moresby rift, specifically in the earliest sediments that fill the space created by the graben-bounding faults. None of the Leg 180 sites targeted the earliest rift sediments because they occur at ~2500 mbsf in Moresby rift and at >1500 mbsf on Moresby Seamount (Fig. **F8**). We can, however, correlate the seismic horizons dated at Sites 1109, 1115, and 1118 around the regional grid of seismic profiles and into the Moresby rift. This correlation shows that the early rift sediments are older than 5.5 Ma but younger than the prograding clinoforms beneath the 8.4-Ma unconformity. This unconformity may therefore reasonably be correlated with rift onset, even though we recognize that it has a eustatic component.

F8. Interpreted line drawing of MCS profile, p. 34.

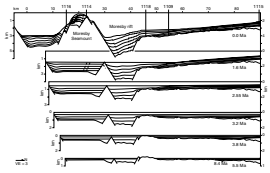

Note that Moresby Seamount was not a topographic high in the late Miocene. It was part of a wide graben system that included what is now Moresby rift as well as the basin to the south of Moreseby Seamount (Figs. F3, F8). All the master faults that currently bound these basins were formed early in the rift history. Some differential sedimentation and tilting, characteristic of half-graben, are evidenced in the earliest rifts and also in the recent (sediment starved) phases of the deformation. At Sites 1114 and 1117 we drilled the south- and north-dipping faults, respectively, that initially delimited a horst block within the wider rift. The basement high drilled at Site 1118 was just north of the graben. Although there were several rifts active farther south at this time, there were none farther north except for a narrow half-graben near ~9°S that continued to reactivate a forearc structure (Fig. F3).

PLIOCENE SUBSIDENCE, SEDIMENTATION, AND PALEOENVIRONMENT

Seismic profiles show that a thick sequence of sediments filled the rift basins in the late Miocene and early Pliocene (Fig. F8) (e.g., Goodliffe et al., 1999), though Sites 1108, 1114, and 1116 did not penetrate to these levels. On the northern margin, shallow-marine mixed carbonate-siliciclastic sediments from Sites 1109 and 1115 record gradual subsidence of shelf basins in the early Pliocene (Shipboard Scientific Party, 1999). The northward-flowing Miocene drainage was reversed as the margin thinned and subsided southward toward the active rifts. The transition at ~50 mbsl from inner to outer neritic paleowater depths occurred first at Site 1109 (~4.9 Ma) and slightly later at Site 1115 (~4.6 Ma) (Fig. F7).

In the early Pliocene, however, basins on the northern shelf were somewhat isolated from the rift basins farther south, as evidenced by sediments lapping onto the Site 1118 basement high (and lateral equivalents). The shelf deposits formed lensoid stratal packages until ~3.2 Ma (Fig. F8) (**Goodliffe et al.,** this volume; Fang, 2000). We mentioned above that thermal subsidence following previous forearc extension may have produced this accommodation space. Alternatively, or in addition, the flanks of the active rifts may have been uplifted and backtilted as the footwalls to the graben-bounding faults were unloaded, thereby providing a southern border to the shelf basins that were gradually subsiding concomitant with regional crustal thinning. The paleochannel drilled at Site 1109 (Goodliffe et al., 1999) transected this rift-flank and outer-shelf high, locally connecting the shelf and rift basins.

Benthic foraminifers provide a detailed record of the continued margin subsidence, with Site 1109 passing ~150 mbsl (i.e., from outer neritic to upper bathyal) at ~4.2 Ma, followed by Site 1115 at ~3.8 Ma (Fig. F7) (Shipboard Scientific Party, 1999). Site 1118 was finally drowned at this time (~3.8 Ma) and quickly passed to upper bathyal depths (~3.6 Ma) as the margin deepened southward (Shipboard Scientific Party, 1999). As Site 1118 drowned, shallow-water bioclastic debris with Sr isotopic ages of 11.3–13.6 Ma was redeposited in early Pliocene limestones there (**Allan et al.,** this volume) above fluvial conglomerates with prevalent dolerite and rare gabbro clasts (Shipboard Scientific Party, 1999; **Cortesogno et al.,** this volume). Rapid slope sedimentation and even faster subsidence occurred at all three sites after 3.8 Ma (Fig. F7). The pattern of shingled onlap of near-horizontal and thicker rift-proximal

sediments with the northern margin slope sediments was established by 3.8 Ma and continued to ~1.2 Ma (Fig. F8) (**Goodliffe et al.,** this volume). The northern margin sediments record a marked decrease in magnetic susceptibility and the concentration of magnetite at 3.8 Ma, coincident with the increased sedimentation rates associated with the onlapping sediments (Ishikawa and Frost, in press).

The paleorift basin Sites 1108, 1114, and 1116, as well as the northern margin Sites 1109, 1115, and 1118, yielded their most complete stratigraphic records from middle and late Pliocene times. The siliciclastic deposition was largely from turbidity currents. Higher-energy environments in the rift basins than on the margins are evidenced by high-angle tabular cross-lamination in sandstones and intraformational rip-up clasts, whereas classic Bouma sequences and cross/convolute laminations in clay to fine sandstones are common to both regions (Shipboard Scientific Party, 1999; Robertson et al., 2001; **Cortesogno et al.,** this volume). Sites 1108, 1114, and 1116 were all at mid-bathyal water depths (>500 ± 100 mbsl) at 3.4 Ma, whereas the northern margin sites did not subside through these water depths until 2.6 Ma (Fig. F7). Sites 1114 and 1116 remained mid-bathyal throughout the Pliocene. Site 1108 passed into lower-bathyal depths by 3.2 Ma (>900 mbsl) (J. Resig, pers. comm., 2001), some 500 m deeper and ~5 km southeast along the Moresby rift axis from the section depicted in Figure F8.

Awadallah et al. (this volume) performed a detailed analysis using Formation MicroScanner (FMS) and core data of the turbidite facies and bed-thickness characteristics of the Pliocene sections in the three northern margin sites. They found that the number of sand and silt turbidites decreases approximately exponentially with increasing bed thickness and that there is a significant "tail" of relatively thick beds. The frequency of sand and silt turbidite deposition decreases upslope from Site 1118 to 1109 to 1115, probably as a result of lateral and distal fining (and subsequent bioturbation of the fines). The turbidite bed thicknesses fit a power-law model, with exponential distributions of the number of beds thicker than a constant times the exponent thickness. Awadallah et al. propose that the underlying control on this pattern is the well-known power-law distribution of earthquakes—a model that seems very feasible in this region of active rifting (Fig. F2). Sites 1109 and 1118 show segmented power-law fits, with the exponent constant being greater for thicker than thinner beds. They explain this following Malinverno (1997), who showed that natural bed-thickness data sets can be expected to plot as segmented linear trends with different slopes if there is a relationship between bed length and bed thickness that depends on the bed volume. For example, smaller flows and their deposits might be confined by topographic features such as the channel in which Site 1109 was drilled, whereas larger flows might be free to spread over wider areas.

Rates of clastic input and sedimentation decrease after 3.2 Ma at the northernmost Site (1115), and there is a concomitant increase (to the present) in carbonate content with the increasing proportion of pelagics (Shipboard Scientific Party, 1999; **Cortesogno et al.,** this volume; **Robertson and Sharp,** this volume). At Site 1109 the corresponding change (increasing pelagics and hence carbonate) did not occur until ~1.2 Ma. A marked increase in magnetic susceptibility and the concentration of magnetite at 3.2 Ma at Site 1115 reflects a change in source material and/or supply route (Ishikawa and Frost, in press). This change appeared slightly earlier at Sites 1118 (3.4 Ma) and 1109 (3.3 Ma), indicating northward onlap (Ishikawa and Frost, in press).

The provenance of the mixed clastic sediments is multifold. The lithic mineralogy of the sandstones and geochemical data on clay-mudstones and tephra reveal that the clastics were derived from calc-alkaline volcanics plus pelitic metamorphic rocks and lesser ultramafic rocks (Shipboard Scientific Party, 1999; Lackschewitz et al., 2001; Robertson et al., 2001; **Cortesogno et al.,** this volume; **Robertson and Sharp,** this volume; **Sharp and Robertson,** this volume). These components have nearby source exposures on the Papuan Peninsula and D'Entrecasteaux Islands (Fig. **F2**). There are also Pliocene andesites on the Amphlett Islands and Egum Atoll, and 1- to 2-Ma trachytes on the Lusancay Islands (Smith and Milsom, 1984). Coalified wood fragments in the recovered sediments reveal that source terranes included eucalyptus forested uplands subject to forest fires (**Cook and Karner,** this volume). In addition, high-K volcanic ash layers and muds rich in tephra that appear at Sites 1109 and 1115 at <2.3 Ma are indicative of explosive eruptions from rhyolitic volcanoes of the D'Entrecasteaux Islands, both peralkaline (Dawson Strait) and calc-alkaline (Moresby Strait) (Lackschewitz et al., 2001; **Robertson and Sharp,** this volume; Stoltz et al., 1993).

The emergence of the D'Entrecasteaux Islands, associated with the buoyant emplacement of metamorphic core complexes in a continental arc rifting environment (Baldwin et al., 1993; Martinez et al., 2001), shed voluminous coarse debris along strike from the Moresby rift, as evidenced by the Pliocene conglomerates and sandstones at the proximal Goodenough 1 well and the sandstones, siltstones, and interlayered limestones at the more distal Nubiam 1 well (Fig. **F4**) (Francis et al., 1987). Most of the ophiolitic cover rocks were eroded during the unroofing and exposure of the metamorphic (and granodioritic) cores (Davies and Warren, 1988; Hill, 1994).

Interpretation of seismic profiles between Sites 1109 and 1115 indicates that another source of sediment since ~3.2 Ma was slumping of and erosion from the northern margin slopes (**Goodliffe et al.,** this volume). Approximately 40 m of Pliocene sediment was redeposited in Pleistocene slumps, and there is a significant component of reworked slope sediments at Site 1109 (Resig and Frost, 2001). These processes continue today, as evidenced by headwall scars and submarine channels eroding the area (Fig. **F2**). In addition to this downslope sedimentation, there is evidence for dominantly along–basin axis flow in the Pliocene. The orientation of the subhorizontal maximum axes of the ellipsoids of the magnetic susceptibility (corrected for bedding dip and core orientation) between 490 and 680 mbsf (middle Pliocene) at Site 1118 suggest an east-southeast–west-northwest–directed paleocurrent during sedimentation, almost perpendicular to the present-day slope (Shipboard Scientific Party, 1999).

Siesser (this volume) studied the relative abundance of two temperature-diagnostic nannofossil species to identify Pliocene surface water temperature trends at Site 1115. He shows that surface waters were mostly warm during the early Pliocene until a cool interval at ~3.2 Ma. A return to warm conditions at 3–2.8 Ma was followed by another cool interval at 2.6–2.4 Ma, a warm event at 2.3 Ma, and then a decline at 2.2 Ma to sustained cool conditions reflecting Northern Hemisphere glaciation.

QUATERNARY RIFTING AND SEDIMENTATION

The Pleistocene paleogeography and environment, being similar to the present, is the easiest to envision, but it is significantly different from that of the Pliocene. A Quaternary carbonate platform developed on the Trobriand forearc west of 151°1′E (Fig. F2), replacing the formerly siliciclastic deposition there. It is represented by the Kiriwina Limestone in the Goodenough 1 and Nubiam 1 wells (Fig. F4). East of 151°10′E, the northern margin continued to subside in middle bathyal water depths (Fig. F7), outpacing any possible reef growth except along the outer forearc high (the Trobriand-Woodlark trend) and around Pliocene volcanic centers such as Egum Atoll (Fig. F2). The rift-onset erosional unconformity, which was at sea level at 8.4 Ma, is now under ~0.8 km of sediments and 2.2 km of water on the northern rift flank in the vicinity of Site 1109 and is buried beneath ~2.5 km of sediments in the ~3-km water depths of Moresby rift (Fig. F8).

That the middle and late Pliocene sediment compositions and depositional styles at Sites 1114 and 1116 on Moresby Seamount are very similar to those of Site 1108 at Moresby rift supports the inference that all three sites were in laterally connected depositional basins during Pliocene time (Robertson et al., 2001). In contrast, movement in the Pleistocene on the normal faults that bound Moresby Seamount uplifted the footwall Seamount and lowered the hanging-wall rift basins such that these sites are no longer in depositional continuity (Fig. F8). This isolation by faulting is younger than the late Pliocene deposition at Sites 1114 and 1116 (Figs. F6, F7) and so must have occurred in the Pleistocene. Furthermore, terrigenous sediments ceased to reach Sites 1109 and 1115 during the Pleistocene (**Robertson and Sharp,** this volume) (note, the Quaternary section was drilled without coring at Site 1118). The significant decrease in sedimentation rates seen in the sediment and seismic stratigraphies at the northern margin sites, as well as at Moresby rift Site 1108, occurred at ~1.2 Ma (Figs. F7, F8) (**Goodliffe et al.; Takahashi et al.,** both this volume). We infer that rift faulting had sufficiently changed the depositional pathways so as to isolate these sites from all but local clastic input by this time.

Structural analysis of core and FMS borehole images from Site 1114 indicates an oblique extensional system on Moresby Seamount, with differential rotation of strata within fault-bounded blocks (**Louvel et al.,** this volume). Nevertheless, the strata dominantly dip 10°–40° northwest, and the tectonic breccia at the faulted sediment-basement contact dips ~60° southwest, consistent with the seismic reflection data (e.g., Fig. F8) (**Louvel et al.,** this volume; Goodliffe et al., 1999).

Given that at the longitude of Moresby Seamount nearly all seismicity is focused on Moresby rift, it is reasonable to consider the implications of focusing all the recent extension there and to compare this estimate with that derived from observed offsets on the rift-bounding faults. Using the Woodlark Basin opening poles of Taylor et al. (1999), we obtain an average extension rate of 37 mm/yr along azimuth 355° over the last 1.2 Ma at Moresby rift (specifically, at 9.7°S, 151.6°E)—a value that is well constrained by the seafloor-spreading magnetic anomalies farther east. For comparison, the total basement offset on the Moresby normal fault is ~10 km horizontally and 5 km vertically (which equates to 11 km at 27° dip), and the corresponding offsets on the northern antithetic fault of the Moresby rift are 1.5 km horizontally and vertically. One-third of the total 11.5 km of horizontal extension

represented by the Moresby rift north of Moresby Seamount occurred early in the rift history (8.4–3.8 Ma) (Fig. F8). Therefore, <220 k.y. is required to account for the other 8 km of horizontal offset if the full extension rates typical of the last 1.2 Ma (37 mm/yr) are applied.

We do not propose that all the extension over this period was focused on Moresby rift alone. For example, the faults bounding the basin south of Moresby Seamount probably accounted for a similar amount of extension during this time. It is clear, however, that with most of the total opening focused ahead of the seafloor spreading tip (i.e., around Moresby Seamount), vertical motions associated with extensional faulting will have radically changed the local topography and sedimentation. Examples of these effects have been mentioned above, including the uplift and isolation of Moresby Seamount and the cessation of sediment onlap onto the northern margin.

Other than pelagics, Quaternary sedimentation in Moresby rift has been limited to talus derived from fault scarps plus sediments eroded from the northern margin, as confirmed at Sites 1108 and 1110–1113 (Shipboard Scientific Party, 1999). A detailed oxygen isotope and nannofossil taxonomic study of surface sediments at the northern margin Site 1109 revealed that the top 17 mbsf were deposited in 195 k.y. and that the relative abundance of species is consistent with the waxing and waning of the Western Pacific Warm Pool in phase with interglacial and glacial cycles (Takahashi and Okada, in press).

DIAGENESIS AND PHYSICAL PROPERTIES OF SEDIMENTS

Extensive sampling and logging of several holes on the downflexed northern margin of the Moresby rift basin allowed the processes of sediment compaction and diagenesis to be studied. One of the puzzling observations made during Leg 180 is the occurrence of zones of high porosity that deviate from the classical exponential decrease with depth. These zones of high porosity are of special interest since they are potentially affected by overpressure (Shipboard Scientific Party, 1999). By comparing simulated porosity changes with measured porosity data, Stover et al. (in press) argue that poroelastic deformation is likely to be the dominant mechanism for compaction, whereas viscoelastic compaction may significantly contribute in areas of high porosities. At Site 1109, the analytical solutions developed by Stover et al. allow one to predict overpressures of the order of 1 MPa only in the high-porosity zones, a result confirmed by **Kemerer and Screaton** (this volume) at Site 1108. Therefore, significant overpressures do not seem—from these theoretical results—to occur. In addition, lithology appears to exert a strong control on permeability, since the reported value of 10^{-16} m^2 in a sand layer at Site 1108 (**Kemerer and Screaton,** this volume) is ~20 times larger than the value in silty claystones (Bolton et al., 2000). Kemerer and Screaton suggest that lateral fluid migration in such sandy layers, whose occurrence is common, may be an efficient way to lower pressures within the basin.

ORGANIC AND INORGANIC GEOCHEMISTRY AND MICROBIOLOGY

Studies of organic matter in Leg 180 sediments show that formation temperatures have been insufficient to cause an increase in vitrinite reflectance levels; the variations in reflectance relate mainly to tissue type (**Cook and Karner,** this volume). This suggests that formation temperatures, even in the deeper samples, have not exceeded ~50°C. This is consistent with the results of **Katz** (this volume), who studied the organic geochemistry of samples from Sites 1108 and 1109. Organic carbon and pyrolysis gas chromatographic data indicate that there is no significant source rock potential at Site 1108, although sufficient organic matter (0.6 ± 0.5 wt%) is present to explain the limited gas present within the recovered cores. The decrease in methane/ethane ratios with depth is not associated with an increase in gas abundance (Shipboard Scientific Party, 1999) but can be attributed to a continuum of microbial (and possibly low-temperature [<75°C] nonbiological) processes (**Katz,** this volume). Katz concludes that the hydrocarbons encountered during drilling at Site 1108 appear to be indigenous and not a migrated product or contaminant, suggesting that the location can be revisited safely.

In contrast, the organic-rich (1.5–33 wt%) lagoonal facies near the base of Site 1109 contains zones with significant hydrocarbon potential. However, several independent lines of evidence indicate that it is thermally immature. This evidence includes pyrolysis thermal maturation indexes, the relative abundance and overall composition of the bitumen (or total organic extract), the nature of the saturated hydrocarbon fraction gas chromatograms, and the vitrinite reflectance levels (**Katz; Cook and Karner,** both this volume). Likewise, **Mather et al.** (this volume), using purge-trap adsorption gas analysis, detected increased concentrations of hexane and 2-methyl- and 3-methylpentane in this facies at both Sites 1109 and 1115. They ascribe this formation of branched low molecular weight hydrocarbons to low-temperature bacterial processes, possibly enhanced at these levels by the more terrigenous nature of the organic matter (with potentially more isoprene polymers than marine-derived organic matter).

New sterile, anoxic sampling techniques for handling indurated (rotary cored) sediments allowed Leg 180 scientists to set the current subseafloor depth record for the known biosphere. Culturable anaerobic bacteria and realistic rates of anaerobic bacterial activity (sulfate reduction, methanogenesis, and thymidine incorporation) are present in the deepest samples from the subseafloor biosphere analyzed to date. Microbial populations occur at 842 mbsf at Site 1118, and measurable activities were detected at 800 mbsf at Site 1115 (Fig. **F9**) (Shipboard Scientific Party, 1999; **Wellsbury et al.,** this volume, submitted [**N1**]).

Depth profiles of sulfate, ammonia, methane, and alkalinity indicate that bacterially mediated oxidation of organic matter affects the chemistry of pore fluids from Sites 1109, 1115, and 1118 nearly to the bottom of each drill hole (Fig. **F9**) (Shipboard Scientific Party, 1999). In addition, the presence of sulfate deep within Site 1118 as well as reversals in the ^{18}O and Sr isotope depth profiles indicate that fluid flow is significant there (**De Carlo et al.,** this volume). The other dominant chemical reactions common to the Woodlark Rise sites are diagenesis of metastable biogenic carbonates and alteration of volcanic matter (in the sediments and basement) to authigenic clays (i.e., smectite).

F9. Biogeochemical profiles, p. 35.

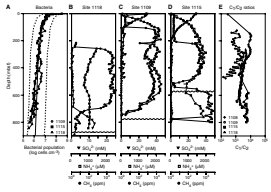

SHALLOW-ANGLE MORESBY NORMAL FAULT

There is now clear evidence that large earthquakes rupture fault planes dipping 23°–35° in the two rift areas (Woodlark and Corinth) where high opening rates (10–37 mm/yr) are accompanied by high seismicity rates (Abers, 2001). Waveform inversion studies place an Mw = 6.2 earthquake with ~32°N dip on the Moresby normal fault at 5.3 km depth (Abers et al., 1997). Water multiples in the seismograms require 3.0 ± 0.2 km of water overlying the source, a condition only fulfilled near the Moresby rift axis (Figs. **F2, F8**). The teleseismic location of this and nearby earthquakes better fits the bathymetry and the location of microseismicity determined by a local array of ocean bottom seismometers/hydrophones (OBS/H) if the teleseismic locations (biased by the presence of velocity anomalies associated with subducted slabs to the north) are shifted south by 15 km (B. Taylor and B.C. Zelt, unpubl. data)—as has been done in Figure **F2**.

In spite of the failure to reach the Moresby detachment at depth (the main objective at Site 1108), critical information was provided by studies of samples from the fault zone where it cropped out at Site 1117. Onboard analyses revealed a transition downward from ductile to brittle conditions beneath the detachment (Shipboard Scientific Party, 1999), but information concerning the conditions at which the associated structures formed is conflicting. Roller et al. (2001) showed that synmylonitic structures and vein fill mineralogy (mostly calcite) indicate exhumation from significant depth. In particular, the quartz-rich porphyroclasts in the mylonite commonly display signs of dynamic recrystallization that attest to ductile creep under (at least) lowermost greenschist facies conditions. The deformation fabrics also show evidence for multiple opening and healing of veins during retrograde evolution and hydrothermal mineralization. Within the veins, calcite twins were used by Roller et al. as empirical paleopiezometers to derive differential paleostresses on the order of 20–40 MPa at temperatures lower than 200°C, corresponding to a maximum depth of 2 km assuming the rift basin thermal gradient of ~100°C/km (Shipboard Scientific Party, 1999). These temperatures and depths are consistent with the observation that the 66-Ma gabbro beneath the fault at Site 1117 was not thermally reset by subsequent rifting events and so must have remained at shallow and cool (<250°C) levels in the crust (**Monteleone et al.,** this volume). However, they are not consistent with the estimated 2.5- to 3-km depth and 250°–300°C temperatures that mark the beginning of plastic deformation evidenced in the mylonites. Furthermore, the differential pressures are not consistent with the fault geometry, which indicates that there was no more than a few hundreds of meters of overburden above Site 1117 prior to faulting. There is consequently a conflict between the estimated depths and temperatures at which the mylonites and calcite twins formed and all other indicators of these parameters at Site 1117. A possible resolution is to invoke a dynamic shear heating process to explain the mylonites and calcite twins.

As briefly stated above (see also Shipboard Scientific Party, 1999), the fault gouge and the mylonites at Site 1117 show evidence of strong hydrothermal mineralization, suggestive of fluid migration within the detachment fault zone. This has been further substantiated by hydraulic conductivity testing on minicores from Sites 1108, 1114, and 1117 (Kopf, 2001). These measurements show that the fault gouge at Site 1117 has a larger permeability (on the order of 10^{-14} m^2), especially in

the direction parallel to the tectonic fabrics, than both the rift basin sediments at Site 1108 and the footwall block basement at Site 1114 (10^{-15} to 10^{-17} m^2). Vertical permeability measurements on samples from Sites 1109 (**Stover et al.,** this volume) and 1108, 1115, and 1118 (**Kemerer and Screaton,** this volume) led to similar values that range from 10^{-16} to 10^{-18} m^2. The increase in permeability in the direction parallel to the fabric obviously derives from shear compaction. Together with the decrease in permeability above the fault zone (due both to the shear fabrics and the cementation), it results in enhanced fluid migration within the fault zone, as well as fluid overpressure that may trigger the fault activity. Note that anisotropic permeability also occurs in fine-grained sediments outside of fault zones at Site 1108, due to aligned microfractures (Bolton et al., 2000).

The detailed study by Floyd et al. (2001) of an MCS profile that images the fault zone at depth (and on which Site 1108 was drilled) provides a completely independent approach to the question of fluid flow within the fault zone. Their inversion of seismic reflection data indicates the occurrence within the fault zone of a 33-m-thick layer with a low *P*-wave velocity (4.3 km/s) at depths between 4 and 5 km. Isolated sections of the fault even show velocities as low as 1.7 km/s that strongly suggest high porosities maintained by high fluid pressures associated with hydrothermal fluid flow within the fault zone. Although the measurement technique as well as the conditions of overburden are quite different, these velocities are even lower than those obtained from core measurements on the fault gouge at Site 1117 (2 km/s) (Shipboard Scientific Party, 1999) and require high porosities and near-lithostatic fluid pressures to maintain them. High porosities are confirmed by the concurrent decrease in Poisson's ratio and *P*-wave velocities in sections of the fault zone (inferred from the amplitude variation with offset of the common midpoint gathers), which is interpreted as a greater decrease in *P*-wave than *S*-wave velocity resulting from slower *P*-wave paths through pore fluids (Floyd et al., 2001).

In addition to the evidence for a permeable and porous Moresby fault zone at greater than hydrostatic pressures, the samples of the gouge from the fault at Site 1117 provide evidence for weak frictional properties. The fault gouge minerology is talc-chlorite-serpentinite-calcite (Shipboard Scientific Party, 1999)—an association commonly produced by alteration of mafic and ultramafic rocks (Deer et al., 1992), such as the gabbros at Site 1117. Talc, more than serpentinite, has the important mechanical property of maintaining low coefficients of friction to greenschist pressures and temperatures (C. Scholz, pers. comm. 2000). Our best estimates of the Moresby fault dip (27°–32°N) (Abers et al., 1997; Taylor et al., 1999) are consistent with the frictional properties expected for mature faults with well-developed gouge zones (Abers, 2001; Byerlee and Savage, 1992). As Abers (2001) demonstrates, very unusual fault mechanics may not be needed. Specifically, a combination of a cohesionless fault with only slightly reduced coefficients of friction (0.5) vs. surrounds with cohesion and typical friction (0.6) permits failure in the upper crust on faults of 20°–35° dip without hydrofracture *even at hydrostatic fluid pressures*.

Thus, the propensity for failure at the shallow dips (~30°) observed on the Moresby normal fault is overdetermined (i.e., the result of several congruent factors, each sufficient to produce the result). There is evidence for both:

1. Fault weakening as a consequence of (a) the high slip rates (the 30- to 37-mm/yr extension is focused on the Moresby rift, as the seismicity shows) and (b) the talc-chlorite-serpentine gouge mineralogy and
2. Enhanced hydrothermal fluid migration within the permeable, porous, and anisotropic fault zone at greater than hydrostatic fluid pressures.

These fault properties and failure modes are a logical consequence of a continent with an ophiolitic upper crust being rapidly extended adjacent to a seafloor spreading center. Such shallow-angle normal faults may be a common feature of strain localization during the transition from rifting to spreading (Abers et al., 1997; Taylor et al., 1999; Floyd et al., 2001; Pérez-Gussinyé and Reston, 2001). In this case, however, given the shallow dips of the opposing faults to either side of Site 1114 (Figs. **F1, F8**), at least one if not both of these faults initiated at shallow dips (i.e., did not rotate from high angles).

FLUID/THERMAL REGIME AND DUCTILE MECHANISMS OF CRUSTAL THINNING

Continental breakup requires thinning the lithospheric mantle and the crust to the point where seafloor spreading can initiate. Constraints on how this thinning has been achieved in the western Woodlark Basin, where Moresby rift is at the point of breakup immediately adjacent to a spreading center (Figs. **F1, F2, F3**), are provided by measurements of crustal structure, strain rate, thermal regime, and upper crustal faulting and subsidence. These data require that a major component of crustal thinning results from flow of the lower crust, that this flow is synrift, and that it may be activated more by fluids than temperature, as discussed below.

That the crust has been thinned is confirmed by a seismic receiver function study that indicates that the crust is 32–42 km thick beneath the Papuan Peninsula and northern Woodlark Rise, but only 20–26 km thick beneath the Goodenough Basin and D'Entrecasteaux Islands (Ferris et al., 2000). The crust thins further to an average thickness of 15–20 km flanking Moresby rift (Zelt et al., 2001).

Based on the Woodlark Basin opening history, strain rates are estimated to have averaged 10^{-14}/s at 151.7°E and could have been one or two orders of magnitude faster when focused on a particular rift (such as immediately preceding breakup) (Taylor et al., 1999). Rifting in the western Woodlark Basin is as fast or faster than anywhere else on Earth today (Abers, 2001) and at least three times as fast as in the Cretaceous separation of Newfoundland from Iberia, for example (Wilson et al., 2001).

In situ measurements of thermal gradients combined with shipboard core measurements of thermal conductivities revealed low heat flow at the northern margin Sites 1115 and 1109 (~30 mW/m^2) that increased rapidly at the rift flank Site 1118 (60 mW/m^2) to relatively high values in Moresby rift Sites 1111 and 1108 (95–100 mW/m^2). These values are consistent with the organic petrology and geochemistry results discussed above. They were confirmed and significantly extended by a pogo-probe heat flow transect, >100 km long, that revealed a quasi-symmetric heat flow anomaly peaking at ~250 mW/m^2 centered over

the basin south of Moresby Seamount and due west of the second spreading segment (Figs. F1, F2, F3) (Martinez et al., 2000; Goodliffe et al., 2000). The heat flow high (where values exceed 100 mW/m²) is 30–40 km wide and tapers southward to values of 40–50 mW/m² on Pocklington Rise (Martinez et al., 2000; Goodliffe et al., 2000).

The locus of breakup and rifting is presently focused on Moresby rift and during the Brunhes Chron included the basin south of Moresby Seamount where the thermal anomaly peaks. Regionally, this location is along the volcanic front of the Trobriand arc, which explains the cooler thermal regime to the north (forearc) than to the south (backarc) (Fig. F3). The reconstructions in Figure F8 summarize the structural and stratigraphic constraints on how the upper crust has stretched in the region of the Leg 180 drilling transect. MCS profiles reveal that the upper crust of the northern margin (Woodlark Rise) has experienced very little extension since rift onset (~1% strain) (e.g., **Goodliffe et al.,** 1999, this volume; Fang, 2000). The small-offset normal faults there occurred late in the rifting history (during the Quaternary) accompanying the long-wavelength downflexing of the margin toward Moresby rift. Nevertheless, the basement, which was near sea level at rift onset at 8.4 Ma, has subsided to >3 km south of Site 1109, equivalent to nearly 3 km of tectonic subsidence if the ~800 m of sediments were to be unloaded (Fig. F8). Simple isostatic calculations show that this requires ~10 km of crustal thinning, which equates to 25%–33% strain for crust initially 40–30 km thick. The total strain since 8.4 Ma over the section shown in Figure F8 is ~33%. Only ~1% strain is evidenced north of Moresby rift, even though the crust may be thinned to 15–20 km (Zelt et al., 2001). How was the long-wavelength subsidence and crustal thinning, which is beyond the influence of faults bounding Moresby rift, achieved in the absence of significant upper crust brittle deformation?

This is another example of the "upper-plate paradox" in which many conjugate rifted margins show evidence of large regional subsidence with little attendant brittle deformation (Driscoll and Karner, 1998). The significant difference in this example is that we know that this phenomenon occurs *synrift,* not just postbreakup. Lower crustal ductile extension can explain this paradox but, for the Woodlark Rise, we also know that the ductile flow is not thermally enabled. The northern margin is cold (~30 mW/m²), having been chilled by the southward subduction of the Solomon Sea plate at the Trobriand Trough. We infer that it is the presence of fluids in the crust (whether derived from Neogene subduction or inherited from the Paleogene ophiolites and subduction) that allows the lower crust to flow out from under the northern margin, causing the northern margin to subside synrift. The lower crustal flow would thus be on a more regional scale than the upper crustal brittle deformation, which is presently focused at the Moresby rift and normal fault.

ACKNOWLEDGMENTS

This synthesis draws on the postcruise work of many Leg 180 scientists and their colleagues. Thanks to Alastair Robertson for leading the insightful postcruise field trip to the analogous extensional provinces of the Menderes and Alasehir graben in western Turkey. Andrew Goodliffe helped produce the figures in this paper. Careful reviews by Hugh Davies and Tim Reston helped to improve the manuscript. The publications staff at ODP-TAMU, especially Gigi Delgado, the coordinator for

this volume, are gratefully acknowledged. So, too, is Adam Klaus, our ever-helpful staff scientist. This research used data provided by the Ocean Drilling Program (ODP). ODP is sponsored by the U.S. National Science Foundation (NSF) and participating countries under management of Joint Oceanographic Institutions (JOI), Inc. Funding for this research was provided by the NSF (in the USA) and CNRS-INSU (in France). This is SOEST contribution No. 5873 and Géosciences azur contribution No. 395.

REFERENCES

Abers, G.A., 2001. Evidence for seismogenic normal faults at shallow dips in continental rifts. *In* Wilson, R.C.L., Whitmarsh, R.B., Taylor, B., and Froitzheim, N. (Eds.), *Non-Volcanic Rifting of Continental Margins: A Comparison of Evidence from Land and Sea*. Spec. Publ.—Geol. Soc. London, 187:305–318.

Abers, G.A., Mutter, C.Z., and Fang, J., 1997. Earthquakes and normal faults in the Woodlark-D'Entrecasteaux rift system, Papua New Guinea. *J. Geophys. Res.,* 102:15301–15317.

Allan, T., Robertson, A.H.F., Sharp, T.R., and Trotter, J., 2001. Data report: Whole-rock $^{87}Sr/^{86}Sr$ composition and apparent strontium isotopic age of limestones from Site 1118, Woodlark Rift Basin, Southwest Pacific (Ocean Drilling Program Leg 180). *In* Huchon, P., Taylor, B., and Klaus, A. (Eds.), *Proc. ODP, Sci. Results,* 180, 1–5 [Online]. Available from World Wide Web: <http://www-odp.tamu.edu/publications/180_SR/VOLUME/CHAPTERS/158.PDF>.

Ashley, P.M., and Flood, R.H., 1981. Low-K tholeiites and high-K igneous rocks from Woodlark Island, Papua New Guinea. *J. Geol. Soc. Aust.,* 28:227–240.

Awadallah, S.A.M., Hiscott, R.N., Bidgood, M., and Crowther, T.E., 2001. Turbidite facies and bed-thickness characteristics inferred from microresistivity (FMS) images of lower to upper Pliocene rift-basin deposits, Woodlark Basin, offshore Papua New Guinea. *In* Huchon, P., Taylor, B., and Klaus, A. (Eds.), *Proc. ODP, Sci. Results,* 180, 1–29 [Online]. Available from World Wide Web: <http://www-odp.tamu.edu/publications/180_SR/VOLUME/CHAPTERS/166.PDF>.

Baldwin, S.L., and Ireland, T.R., 1995. A tale of two eras: Plio–Pleistocene unroofing of Cenozoic and late Archean zircons from active metamorphic core complexes, Solomon Sea, Papua New Guinea. *Geology,* 23:1023–1026.

Baldwin, S.L., Lister, G.S., Hill, E.J., Foster, D.A., and McDougall, I., 1993. Thermochronologic constraints on the tectonic evolution of active metamorphic core complexes, D'Entrecasteaux Islands, Papua New Guinea. *Tectonics,* 12:611–628.

Baldwin, S.L., Montelone, B., Hill, E.J., Ireland, T., and Fitzgerald, P.G., 2000. Continental extension in the western Woodlark Basin, Papua New Guinea. *Eos, Trans. Am. Geophys. Union,* 81:1307.

Berggren, W.A., Kent, D.V., Swisher, C.C., III, and Aubry, M.-P., 1995. A revised Cenozoic geochronology and chronostratigraphy. *In* Berggren, W.A., Kent, D.V., Aubry, M.-P., and Hardenbol, J. (Eds.), *Geochronology, Time Scales and Global Stratigraphic Correlation*. Spec. Publ.—Soc. Econ. Paleontol. Mineral., 54:129–212.

Bolton, A.J., Maltman, A.J., and Fisher Q., 2000. Anisotropic permeability and bimodal pore-size distributions of fine grained marine sediments. *Mar. Petrol. Geol.,* 17:657–672.

Brooks, K., and Tegner, C., 2001. Affinity of the Leg 180 dolerites of the Woodlark Basin: geochemistry and age. *In* Huchon, P., Taylor, B., and Klaus, A. (Eds.), *Proc. ODP, Sci. Results,* 180, 1–18 [Online]. Available from World Wide Web: <http://www-odp.tamu.edu/publications/180_SR/VOLUME/CHAPTERS/155.PDF>.

Byerlee, J.D., and Savage, J.C., 1992. Coulomb plasticity within the fault zone. *Geophys. Res. Lett.,* 19:2341–2344.

Célérier, B., Louvel, V., Le Gall, B., Gardien, V., and Huchon, P., this volume. Presentation and structural analysis of FMS electrical images in the western Woodlark Basin. *In* Huchon, P., Taylor, B., and Klaus, A. (Eds.), *Proc. ODP, Sci. Results,* 180, 1–## [Online]. Available from World Wide Web: <http://www-odp.tamu.edu/publications/180_SR/VOLUME/CHAPTERS/177.PDF>.

Cook, A., and Karner, G.D., this volume. Organic petrology of Leg 180 samples, western Woodlark Basin, Papua New Guinea. *In* Huchon, P., Taylor, B., and Klaus, A. (Eds.), *Proc. ODP, Sci. Results,* 180, 1–36 [Online]. Available from World Wide Web: <http://www-odp.tamu.edu/publications/180_SR/VOLUME/CHAPTERS/157.PDF>.

Cooper, P., and Taylor, B., 1987. Seismotectonics of New Guinea: a model for arc reversal following arc-continent collision. *Tectonics,* 6:53–67.

Cortesogno, L., Gaggero, L., and Gerbaudo, S., 2001. Petrographic contributions to the investigation of volcaniclastic sediments in the western Woodlark Basin, southwest Pacific (ODP Leg 180). *In* Huchon, P., Taylor, B., and Klaus, A. (Eds.), *Proc. ODP, Sci. Results,* 180, 1–43 [Online]. Available from World Wide Web: <http://www-odp.tamu.edu/publications/180_SR/VOLUME/CHAPTERS/159.PDF>.

Davies, H.L., 1980. Folded thrust fault and associated metamorphics in the Suckling-Dayman Massif, Papua New Guinea. *Am. J. Sci.,* 280-A:171–191.

Davies, H.L., and Jaques, A.L., 1984. Emplacement of ophiolite in Papua New Guinea. *In* Gass, I.G., Lippar, S.J., and Shelton, A.W. (Eds.), *Ophiolites and Oceanic Lithosphere*. Spec. Publ.—Geol. Soc., London, 13:341–350.

Davies, H.L., and Smith, I.E., 1971. Geology of eastern Papua. *Geol. Soc. Am. Bull.,* 82:3299–3312.

Davies, H.L., Symonds, P.A., and Ripper, I.D., 1984. Structure and evolution of the southern Solomon Sea region. *BMR J. Aust. Geol. Geophys.,* 9:49–68.

Davies, H.L., and Warren, R.G., 1988. Origin of eclogite-bearing, domed, layered metamorphic complexes ("core complexes") in the D'Entrecasteaux islands, Papua New Guinea. *Tectonics,* 7:1–21.

Davies, H.L., and Warren, R.G., 1992. Eclogites of the D'Entrecasteaux Islands. *Contrib. Mineral. Petrol.,* 112:463–474.

De Carlo, E.H., Lackschewitz, K.K., and Carmody, R., 2001. Data report: Trace element and isotopic composition of interstitial water and sediments from the Woodlark Rise, ODP Leg 180. *In* Huchon, P., Taylor, B., and Klaus, A. (Eds.), *Proc. ODP, Sci. Results,* 180, 1–20 [Online]. Available from World Wide Web: <http://www-odp.tamu.edu/publications/180_SR/VOLUME/CHAPTERS/160.PDF>.

Deer, W.A., Zussman, J., and Howie, R.A., 1992. *An Introduction to the Rock-Forming Minerals* (2nd ed.): London (Longman).

Driscoll, N.W., and Karner, G.D., 1998. Lower crustal extension along the Northern Carnarvon Basin, Australia: evidence for an eastward dipping detachment. *J. Geophys. Res.,* 103:4975–4992.

Fang, J., 2000. Styles and distribution of continental extension derived from the rift basins of eastern Papua New Guinea [Ph.D. dissert.]. Columbia Univ., New York, NY.

Ferris, A., Abers, G., Floyd, J., Lerner-Lam, A., Mutter, J., Craig, M., Davies, H., Sioni, S., and Taylor, B., 2000. Active continental extension and metamorphic core complexes: a PASSCAL seismic deployment in the D'Entrecasteaux Islands, eastern Papua New Guinea. *Eos, Trans. Am. Geophys. Union,* 81:881.

Floyd, J.S., Mutter, J.C., Goodliffe, A.M., and Taylor, B., 2001. Evidence for fault weakness and fluid flow within an active low-angle normal fault. *Nature,* 411:779–783.

Francis, G., Lock, J., and Okuda, Y., 1987. Seismic stratigraphy and structure of the area to the southeast of the Trobriand Platform. *Geo-Mar. Lett.,* 7:121–128.

Goodliffe, A.M., Martinez, F., Taylor, B., Lewis, T.J., Taylor, A.E., and Screaton, E.J., 2000. The geothermal signature of continental breakup: results from the Woodlark Basin. *Eos, Trans. Am. Geophys. Union,* 81:1114.

Goodliffe, A.M., Taylor, B., and Karner, G., 2001. Correlations between seismic, logging, and core data from ODP Leg 180 sites in the western Woodlark Basin. *In* Huchon, P., Taylor, B., and Klaus, A. (Eds.), *Proc. ODP, Sci. Results,* 180, 1–24 [Online]. Available from World Wide Web: <http://www-odp.tamu.edu/publications/180_SR/VOLUME/CHAPTERS/167.PDF>.

Goodliffe, A.M., Taylor, B., and Martinez, F., 1999. Data report: Marine geophysical surveys of the Woodlark Basin region. *In* Taylor, B., Huchon, P., Klaus, A. et al., *Proc. ODP, Init. Repts.,* 180, 1–20 [CD-ROM]. Available from: Ocean Drilling Program, Texas A&M University, College Station, TX 77845-9547, U.S.A.

Haq, B.U., Hardenbol, J., and Vail, P.R., 1988. Mesozoic and Cenozoic chronostratigraphy and cycles of sea-level change. *In* Wilgus, C.K., Hastings, B.S., Kendall,

C.G.St.C., Posamentier, H.W., Ross, C.A., and Van Wagoner, J.C. (Eds.), *Sea-Level Changes—An Integrated Approach.* Spec. Publ.—Soc. Econ. Paleontol. Mineral., 42:72–108.

Harris, C.S., Varol, O., and Mortimer, C.P., 1985. Cape Vogel, Bougainville and New Ireland Basins Report, Appendix II: Biostratigraphy of the Goodenough-1 and Numbiam-1 wells from the Cape Vogel Basin and the L'Etoile-1 well from the Bougainville Basin. Robertson Research (Singapore).

Hegner, E., and Smith, I.E.M., 1992. Isotopic compositions of late Cenozoic volcanics from southeast Papua New Guinea: evidence for multi-component sources in arc and rift environments. *Chem. Geol.,* 97:233–249.

Hill, E.J., 1994. Geometry and kinematics of shear zones formed during continental extension in eastern Papua New Guinea. *J. Struct. Geol.,* 16:1093–1105.

Hill, E.J., and Baldwin, S.L., 1993. Exhumation of high-pressure metamorphic rocks during crustal extension in the D'Entrecasteaux region: Papua New Guinea. *J. Metamorph. Geol.,* 11:261–277.

Hill, E.J., Baldwin, S.L., and Lister, G.S., 1992. Unroofing of active metamorphic core complexes in the D'Entrecasteaux Islands, Papua New Guinea. *Geology,* 20:907–910.

Hill, E.J., Baldwin, S.L., and Lister, G.S., 1995. Magmatism as an essential driving force for formation of active metamorphic core complexes in eastern Papua New Guinea. *J. Geophys. Res.,* 100:10441–10451.

Ishikawa, N., and Frost, G., in press. Rock magnetic properties of sediments from Sites 1109, 1115, and 1118, ODP Leg 180, Woodlark Basin (Papua New Guinea). *Earth, Planets Space.*

Jaques, A.L., and Chappell, B.W., 1980. Petrology and trace element geochemistry of the Papuan ultramafic belt. *Contrib. Mineral. Petrol.,* 75:55–70.

Jaques, A.L., and Robinson, G.P., 1977. The continent/island arc collision in northern Papua New Guinea. *BMR J. Aust. Geol. Geophys.,* 2:289–303.

Katz, B.J., 2001. Geochemical investigation of Sites 1108 and 1109, Leg 180. *In* Huchon, P., Taylor, B., and Klaus, A. (Eds.), *Proc. ODP, Sci. Results,* 180, 1–19 [Online]. Available from World Wide Web: <http://www-odp.tamu.edu/publications/180_SR/VOLUME/CHAPTERS/151.PDF>.

Kemerer, A., and Screaton, E., 2001. Permeabilities of sediments from Woodlark Basin: implications for pore pressures. *In* Huchon, P., Taylor, B., and Klaus, A. (Eds.), *Proc. ODP, Sci. Results,* 180, 1–14 [Online]. Available from World Wide Web: <http://www-odp.tamu.edu/publications/180_SR/VOLUME/CHAPTERS/169.PDF>.

Kopf, A., 2001. Permeability variation across an active low-angle detachment fault, western Woodlark Basin (ODP Leg 180), and its implication for fault activation. *In* Holdsworth, R.E., Strachan, R.A., Magloughlin, J., and Knipe, R.J. (Eds.), *The Nature and Tectonic Significance of Fault Zone Weakening.* Spec. Publ.—Geol. Soc. London, 186:23–41.

Lackschewitz, K.S., Bogard, P.V.D., and Mertz, D.F., 2001. $^{40}Ar/^{39}Ar$ ages of fallout tephra layers and volcaniclastic deposits in the sedimentary succession of the western Woodlark Basin, Papua New Guinea. *In* Wilson, R.C.L., Whitmarsh, R., Taylor, B., and Froitheim, N. (Eds.), *Non-Volcanic Rifting of Continental Margins—A Comparison of Evidence from Land and Sea.* Spec. Publ.—Geol. Soc. London, 187:373–388.

Lister, G.S., and Baldwin, S.L., 1993. Plutonism and the origin of metamorphic core complexes. *Geology,* 21:607–610.

Louvel, V., Le Gall, B., Célérier, B., Gardien, V., and Huchon, P., this volume. Structural analysis of the footwall fault bock of the Moresby detachment (Woodlark rift basin) from borehole images. *In* Huchon, P., Taylor, B., and Klaus, A. (Eds.), *Proc. ODP, Sci. Results,* 180, 1–## [Online]. Available from World Wide Web: <http://www-odp.tamu.edu/publications/180_SR/VOLUME/CHAPTERS/165.PDF>.

Lus, W.Y., McDougall, I., and Davies, H.L., 1998. Emplacement age of the Papuan Ultramafic Belt Ophiolite: constraints from K-Ar and $^{40}Ar/^{39}Ar$ geochronology from

hornblende granulites at the base of the ophiolite near the Musa-Kumusi divide in *Geol. Soc. Austral. Abstracts No. 49*.

Malinverno, A., 1997. On the power law size distribution of turbidite beds. *Basin Res.,* 9:263–274.

Martinez, F., Goodliffe, A.M., Taylor, B., Lewis, T.J., Taylor, A.E., and Screaton, E.J., 2000. Geothermal study of continental rifting in the Woodlark Basin. *Eos, Trans. Am. Geophys. Union,* 81:1114.

Martinez, F., Taylor, B., and Goodliffe, A., 2001. Metamorphic core complex formation by density inversion and lower crust extrusion. *Nature,* 411:930–934.

Mather, I.D., Wellsbury, P., Parkes, R.J., and Maxwell, J.R., 2001. Purge-trap analysis of sediments of the western Woodlark Basin, Sites 1109 and 1115. *In* Huchon, P., Taylor, B., and Klaus, A. (Eds.), *Proc. ODP, Sci. Results,* 180, 1–14 [Online]. Available from World Wide Web: <http://www-odp.tamu.edu/publications/180_SR/VOLUME/CHAPTERS/171.PDF>.

Monteleone, B.D., Baldwin, S.L., Ireland, T.R., and Fitzgerald, P.G., 2001. Thermochronologic constraints for the tectonic evolution of the Moresby Seamount, Woodlark Basin, Papua New Guinea. *In* Huchon, P., Taylor, B., and Klaus, A. (Eds.), *Proc. ODP, Sci. Results,* 180, 1–34 [Online]. Available from World Wide Web: <http://www-odp.tamu.edu/publications/180_SR/VOLUME/CHAPTERS/173.PDF>.

Mutter, J.C., Mutter, C.Z., and Fang, J., 1996. Analogies to oceanic behavior in the continental breakup of the western Woodlark Basin. *Nature,* 380:333–336.

Parkes, R.J., Cragg, B.A., Bale, S.J., Getliff, J.M., Goodman, K., Rochelle, P.A., Fry, J.C., Weightman, A.J., and Harvey, S.M., 1994. A deep bacterial biosphere in Pacific Ocean sediments. *Nature,* 371:410–413.

Pegler, G., Das, S., and Woodhouse, J.H., 1995. A seismological study of the eastern New Guinea and the western Solomon Sea regions and its tectonic implications. *Geophys. J. Int.,* 122:961–981.

Pérez-Gussinyé, M., and Reston, T.J., 2001. Rheological evolution during extension at nonvolcanic rifted margins: onset of serpentinization and development of detachments leading to continental breakup. *J. Geophys. Res.* 106:3961–3975.

Pinchin, J., and Bembrick, C., 1985. Cape Vogel Basin, PNG— tectonics and petroleum potential. In *14th BMR Symposium Extended Abstracts: Petroleum Geology of South Pacific Island Countries*. Bur. Miner. Resour. Aust. Rec., 32:31–37.

Resig, J., and Frost, G., 2001. Micropaleontologic and paleomagnetic approaches to stratigraphic anomalies in rift basins: ODP Site 1109, Woodlark Basin. *In* Wilson, R.C.L., Whitmarsh, R.B., Taylor, B., and Froitzheim, N. (Eds.), *Non-Volcanic Rifting of Continental Margins: A Comparison of Evidence from Land and Sea.* Spec. Publ.—Geol. Soc. London, 187:389–404.

Robertson, A.H.F., and Sharp, T.R., 2002. Geochemical and mineralogical evidence for the provenance of mixed volcanogenic/terrigenous hemipelagic sediments in the Pliocene–Pleistocene Woodlark backarc rift basin, southwest Pacific: Ocean Drilling Program Leg 180. *In* Huchon, P., Taylor, B., and Klaus, A. (Eds.), *Proc. ODP, Sci. Results,* 180, 1–55 [Online]. Available from World Wide Web: <http://www-odp.tamu.edu/publications/180_SR/VOLUME/ CHAPTERS/156.PDF>.

Robertson, A.H.F., Awadallah, S.A.M., Gerbaudo, S., Lackschewitz, K.S., Monteleone, B.D., Sharp, T.R., and the ODP Leg 180 Shipboard Scientific Party, 2001. Evolution of the Miocene–Recent Woodlark Rift Basin, SW Pacific, inferred from sediments drilled during Ocean Drilling Program Leg 180. *In* Wilson, R.C.L., Froitzheim, N., Taylor, B., and Whitmarsh, R.B. (Eds.), *Non-Volcanic Rifting of Continental Margins: A Comparison of Evidence from Land and Sea.* Spec. Publ.—Geol. Soc. London, 187:335–372.

Rogerson, R., Queen, L., and Francis, G., 1993. The Papuan ultramafic belt arc complex. *In* Wheller, G.E. (Ed.), *Islands and Basins: Correlation and Comparison of Onshore and Offshore Geology.* CCOP/SOPAC Misc. Rept., 159:28–29.

Roller, S., Behrmann, J.H., and Kopf, A., 2001. Deformation fabrics of faulted rocks, and some syntectonic stress estimates from the active Woodlark Basin detachment

zone. *In* Wilson, R.C.L., Whitmarsh, R.B., Taylor, B., and Froitzheim, N. (Eds.), *Non-Volcanic Rifting of Continental Margins: A Comparison of Evidence from Land and Sea*. Spec. Publ.—Geol. Soc. London, 187:319–334.

Siesser, W.G., 2001. Pliocene paleoclimatology at ODP Site 1115, Solomon Sea (southwestern Pacific Ocean), based on calcareous nannofossils. *In* Huchon, P., Taylor, B., and Klaus, A. (Eds.), *Proc. ODP, Sci. Results,* 180, 1–14 [Online]. Available from World Wide Web: <http://www-odp.tamu.edu/publications/180_SR/VOLUME/CHAPTERS/154.PDF>.

Sharp, T.R., and Robertson, A.H.F., 2002. Petrography and provenance of volcaniclastic sands and sandstones recovered from the Woodlark rift basin and Trobriand forearc basin, Leg 180. *In* Huchon, P., Taylor, B., and Klaus, A. (Eds.), *Proc. ODP, Sci. Results,* 180, 1–66 [Online]. Available from World Wide Web: <http://www-odp.tamu.edu/publications/180_SR/VOLUME/CHAPTERS/176.PDF>.

Shipboard Scientific Party, 1999. Leg 180 summary. *In* Taylor, B., Huchon, P., Klaus, A., et al., *Proc. ODP, Init. Repts.,* 180: College Station, TX (Ocean Drilling Program), 1–77.

Smith, I.E.M., 1976. Peralkaline rhyolites from the D'Entrecasteaux Islands, Papua New Guinea. *In* Johnson, R.W. (Ed.), *Volcanism in Australasia:* Amsterdam (Elsevier), 275–285.

Smith, I.E.M., 1982. Volcanic evolution in eastern Papua. *Tectonophysics,* 87:315–333.

Smith, I.E.M., and Davies, H.L., 1976. Geology of the southeast Papuan mainland. *BMR J. Aust. Geol. Geophys.,* 165.

Smith, I.E.M., and Milsom, J.S., 1984. Late Cenozoic volcanism and extension in eastern Papua. *In* Kokelaar, B.P., and Howells, M.F. (Eds.), *Marginal Basin Geology.* Spec. Publ.—Geol. Soc. London, 16:163–171.

Stolz, A.J., Davies, G.R., Crawford, A.J., and Smith, I.E.M., 1993. Sr, Nd and Pb isotopic compositions of calc-alkaline and peralkaline silicic volcanics from the D'Entrecasteaux Islands, Papua New Guinea, and their tectonic significance. *Mineral. Petrol.,* 47:103–126.

Stover, S.C., Ge, S., and Screaton, E.J., in press. A one-dimensional analytically-based approach for studying poroelastic and viscoplastic consolidation: application to Woodlark Basin, Papua New Guinea. *J. Geophys. Res.*

Stover, S.C., Screaton, E.J., Likos, W.J., and Ge, S., 2001. Data report: Hydrologic characteristics of shallow marine sediments of Woodlark Basin, Site 1109. *In* Huchon, P., Taylor, B., and Klaus, A. (Eds.), *Proc. ODP, Sci. Results,* 180, 1–22 [Online]. Available from World Wide Web: <http://www-odp.tamu.edu/publications/180_SR/VOLUME/CHAPTERS/168.PDF>.

Takahashi, K., and Okada, H, in press. Paleoceanography for the last 195,000 years in the Solomon Sea (ODP Site 1109) by means of calcareous nannofossils. *Mar. Micropalentol.*

Takahashi, K., Cortese, G., Frost, G.M., Gerbaudo, S., Goodliffe, A.M., Ishikawa, N., Lackschewitz, K.S., Perembo, R.C.B., Resig, J.M., Siesser, W.G., Taylor, B., and Testa, M., 2001. Summary of revised age assignments for ODP Leg 180. *In* Huchon, P., Taylor, B., and Klaus, A. (Eds.), *Proc. ODP, Sci. Results,* 180, 1–12 [Online]. Available from World Wide Web: <http://www-odp.tamu.edu/publications/180_SR/VOLUME/CHAPTERS/152.PDF>.

Taylor, B., 1999. Background and regional setting. *In* Taylor, B., Huchon, P., Klaus, A., et al., *Proc. ODP, Init. Repts.,* 180, 1–20 [CD-ROM]. Available from: Ocean Drilling Program, Texas A&M University, College Station, TX 77845-9547, U.S.A.

Taylor, B., and Exon, N.F., 1987. An investigation of ridge subduction in the Woodlark-Solomons region: introduction and overview. *In* Taylor, B., and Exon, N.F., *Marine Geology Geophysics, and Geochemistry of the Woodlark Basin—Solomon Islands.* Circum-Pac. Counc. Energy Mineral Resour., Earth Sci. Ser., 7:1–24.

Taylor, B., Goodliffe, A., Martinez, F., and Hey, R., 1995. A new view of continental rifting and initial seafloor spreading. *Nature,* 374:534–537.

Taylor, B., Goodliffe, A.M., and Martinez, F., 1999. How continents break up: insights from Papua New Guinea. *J. Geophys. Res.,* 104:7497–7512.

Tjhin, K.T., 1976. Trobriand Basin exploration, Papua New Guinea. *APEA J.,* 81–90.

Walker, D.A., and McDougall, I., 1982. $^{40}Ar/^{39}Ar$ and K-Ar dating of altered glassy volcanic rocks: the Dabi Volcanics. *Geochim. Cosmochim. Acta,* 46:2181–2190.

Weissel, J.K., Taylor, B., and Karner, G.D., 1982. The opening of the Woodlark Basin, subduction of the Woodlark spreading system, and the evolution of northern Melanesia since mid-Pliocene time. *Tectonophysics,* 87:253–277.

Weissel, J.K., and Watts, A.B., 1979. Tectonic evolution of the Coral Sea Basin. *J. Geophys. Res.,* 84:4572–4582.

Wilson, R.C.L., Manatschal, G., and Wise, S., 2001. Rifting along non-volcanic passive margins: stratigraphic and seismic evidence from the Mesozoic of the Alps and Western Iberia. *In* Wilson, R.C.L., Whitmarsh, R.B., Taylor, B., and Froitzheim, N. (Eds.), *Non-Volcanic Rifting of Continental Margins: A Comparison of Evidence From Land and Sea*. Spec. Publ.—Geol. Soc. London, 187:429–452.

Wellsbury, P., Mather, I.D., and Parkes, R.J., 2001. Subsampling RCB cores from the western Woodlark Basin (ODP Leg 180) for microbiology. *In* Huchon, P., Taylor, B., and Klaus, A. (Eds.), *Proc. ODP, Sci. Results,* 180, 1–12 [Online]. Available from World Wide Web: <http://www-odp.tamu.edu/publications/180_SR/VOLUME/CHAPTERS/175.PDF>.

Wellsbury, P., Mather, I., and Parkes, R.J., submitted. Geomicrobiology of low organic carbon sediments in the Woodlark Basin (ODP Leg 180): *FEMS Microbiology Ecology.*

Zelt, B.C., Taylor, B., and Goodliffe, A.M., 2001. 3-D velocity structure at the rift tip in the western Woodlark Basin. *Geophys. Res. Lett.,* 28:3015–3018.

Figure F1. Major physiographic features and active plate boundaries of the Woodlark Basin region. The stippled area encloses oceanic crust formed during the Brunhes Chron at spreading rates labeled in millimeters per year. MT and ST = Moresby and Simbo transform faults, respectively, DE = D'Entrecasteaux Islands. Vertical bar locates Leg 180 drilling transect. Inset is the geographical location of the Woodlark Basin. Lower panels show nested meridional cross sections at 151°34.5′E: (**A**) regional bathymetry and (**B**) local structures across the incipient conjugate margins. Leg 180 drill sites are projected on the B section. Drilled basement types are labeled: D = dolerite, G = gabbro. VE = vertical exaggeration. M.S. = Moresby Seamount.

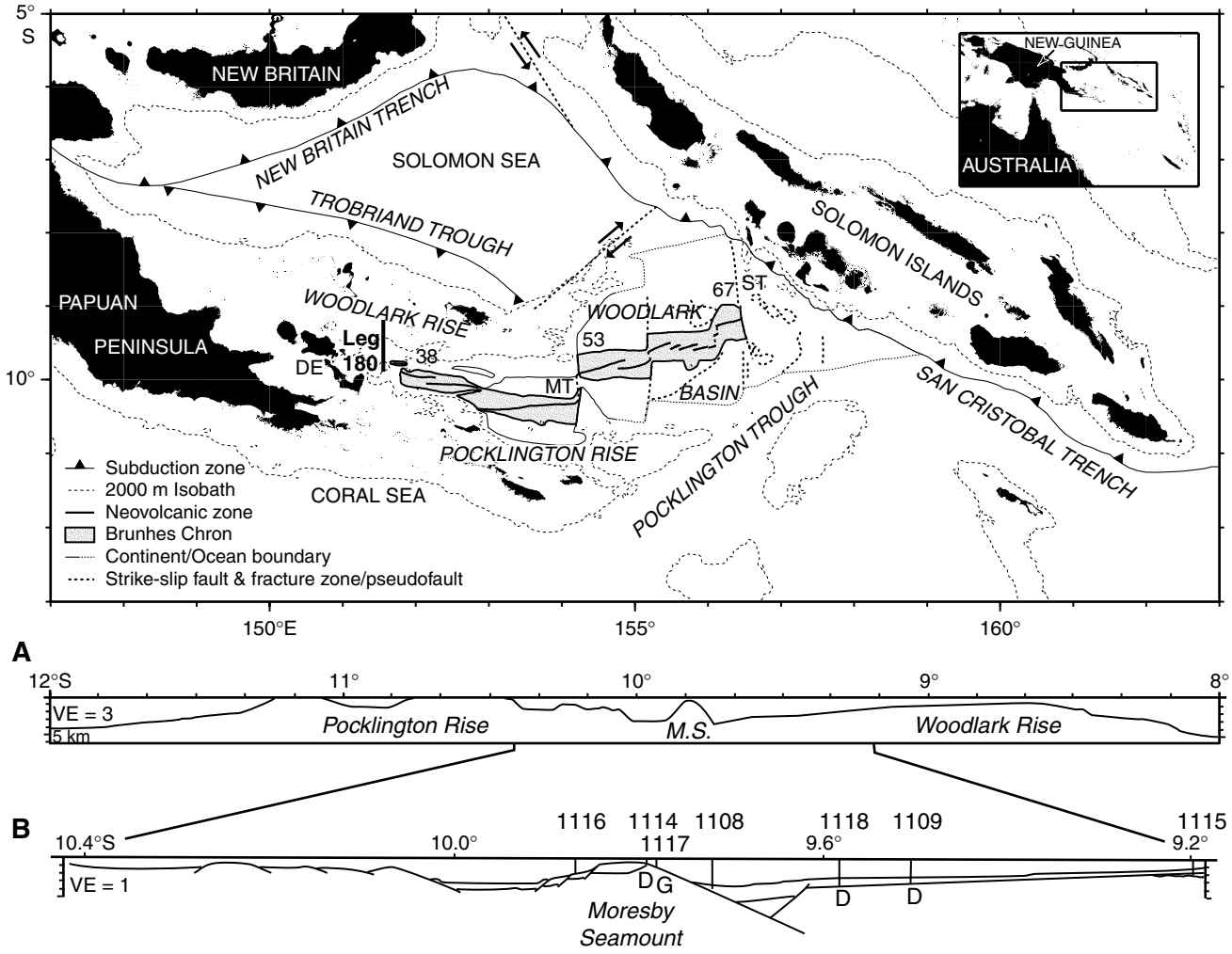

Figure F2. Topography and bathymetry (contours labeled in kilometers) in the region of the Leg 180 drilling transect, showing epicenters and focal mechanisms from Abers et al. (1997) relocated 15 km south in accord with microseismicity data (see **"Shallow-Angle Moresby Normal Fault,"** p. 16). The thin double lines locate the spreading axes (Taylor et al., 1995). G = Goodenough 1 well, N = Numbiam 1 well.

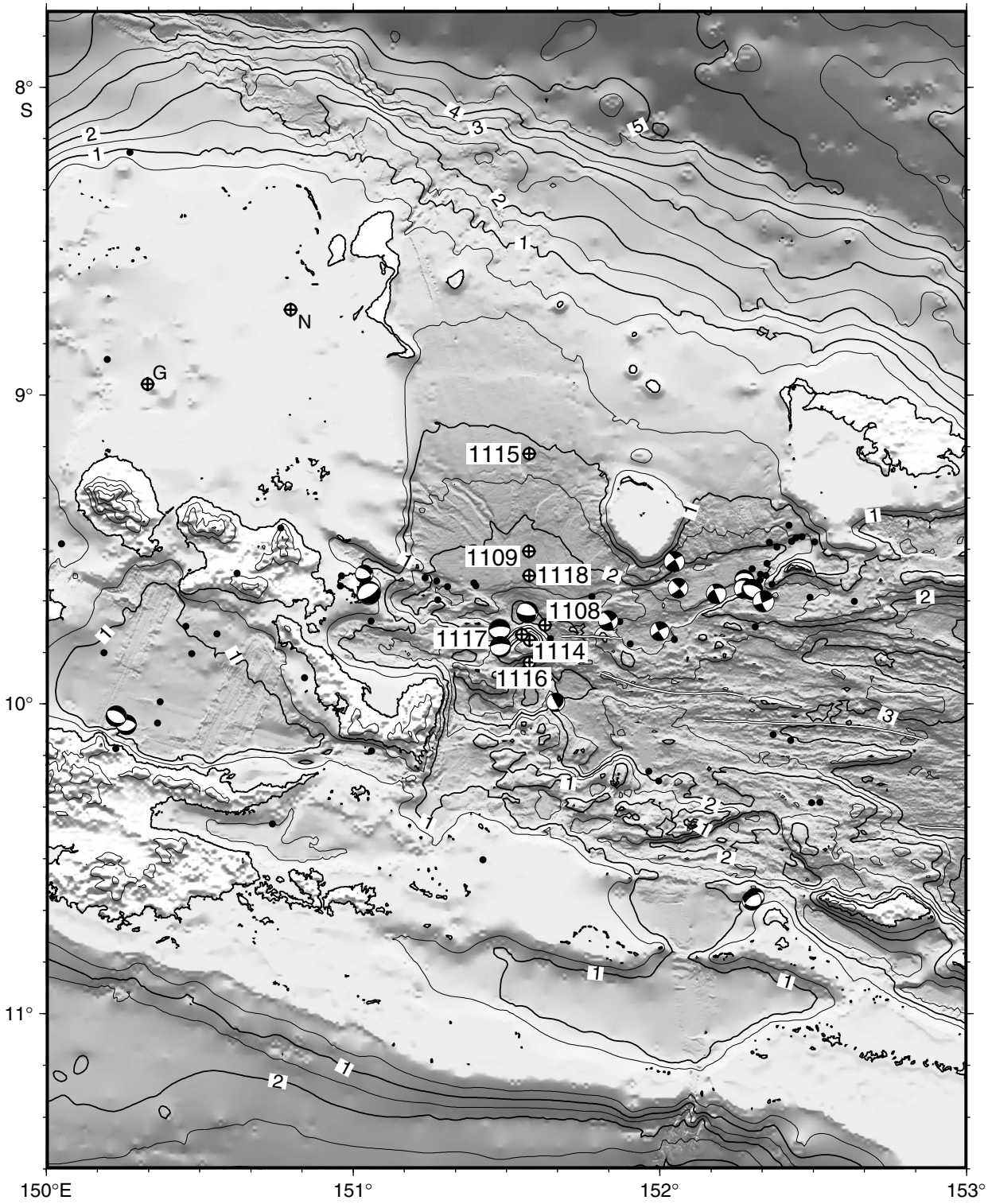

Figure F3. Simplified regional geology, including offshore faults and depocenters. Small circles locate active volcanoes, including Mt. Lamington (L), Mt. Victory (V), and Dawson Strait (D). The dashed line locates the landward boundary of oceanic crust, and the thin double lines locate the spreading axes. Ticks on normal faults indicate the downthrown side; triangles on reverse faults, the upthrusted side. Islands include Amphlett (A), D'Entrecasteaux (DE), Egum Atoll (E), Lusancay (LC), Misima (MI), Trobriand (T), and Woodlark (W). *M* = Moresby Strait, *MR* = Moresby rift, *MS* = Moresby Seamount.

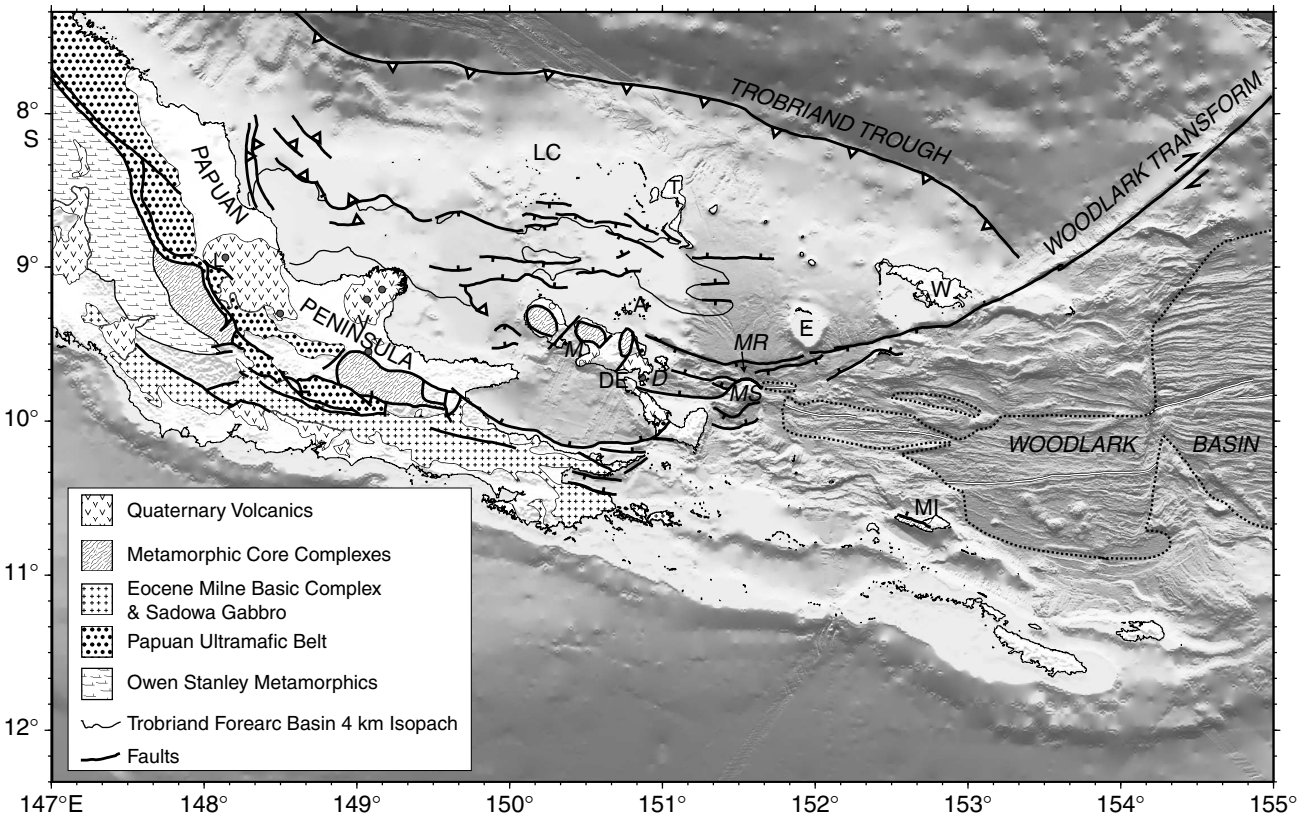

Figure F4. Well correlation diagram, Goodenough 1 to Nubiam 1, showing the biostratigaphy, lithologies, and regional unconformities. Modified after Francis et al. (1987).

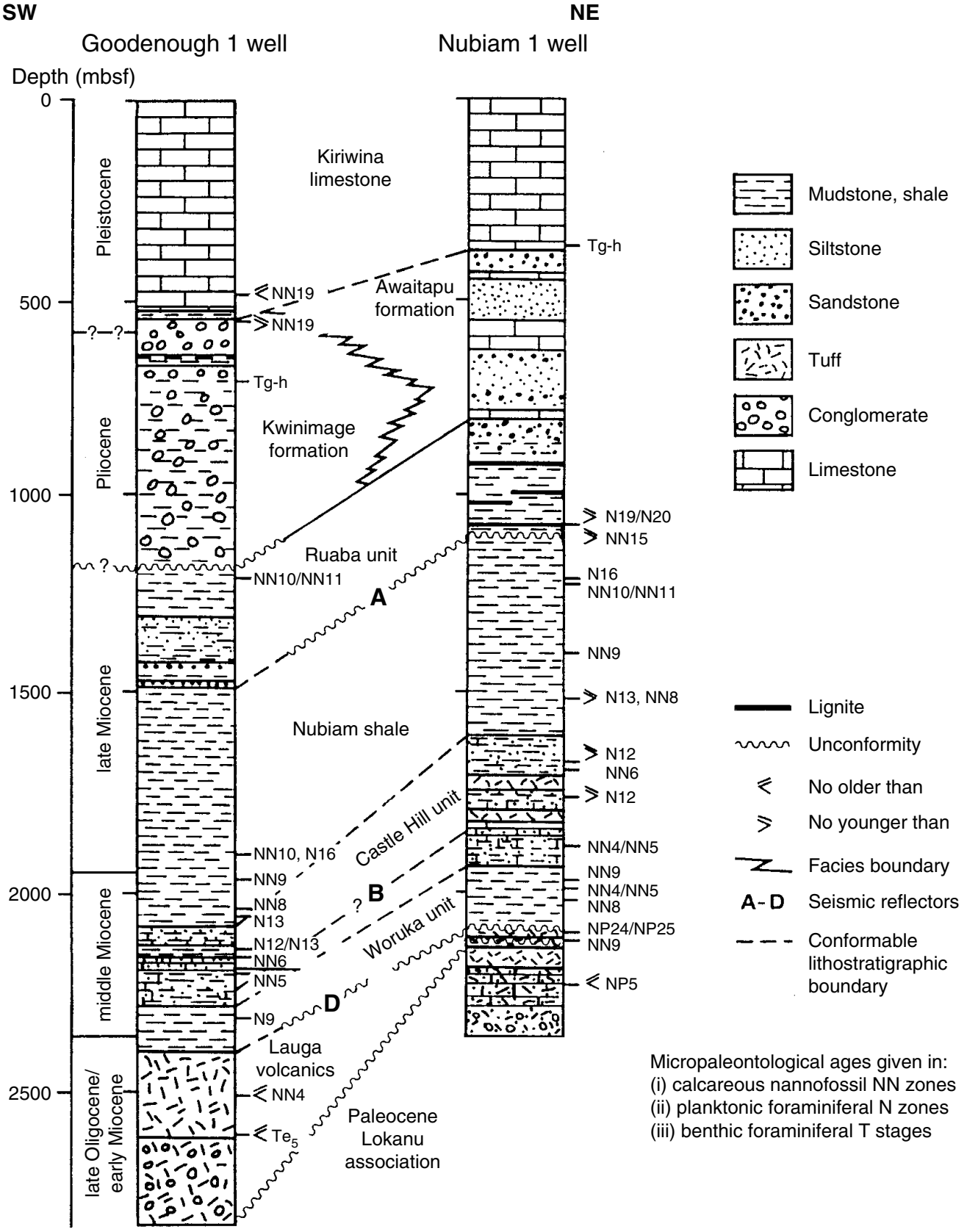

Figure F5. Sedimentation curves at the Goodenough 1 and Nubiam 1 wells, based on nannofossil (square) and planktonic foraminifer (circle) datum events and lithostratigraphic correlation (star), derived from Harris et al. (1985). Dashed lines locate the levels of regional unconformity "A" (see Fig. F4, p. 30). Shown below are paleobathymetry ranges estimated from benthic foraminifers (Harris et al., 1985).

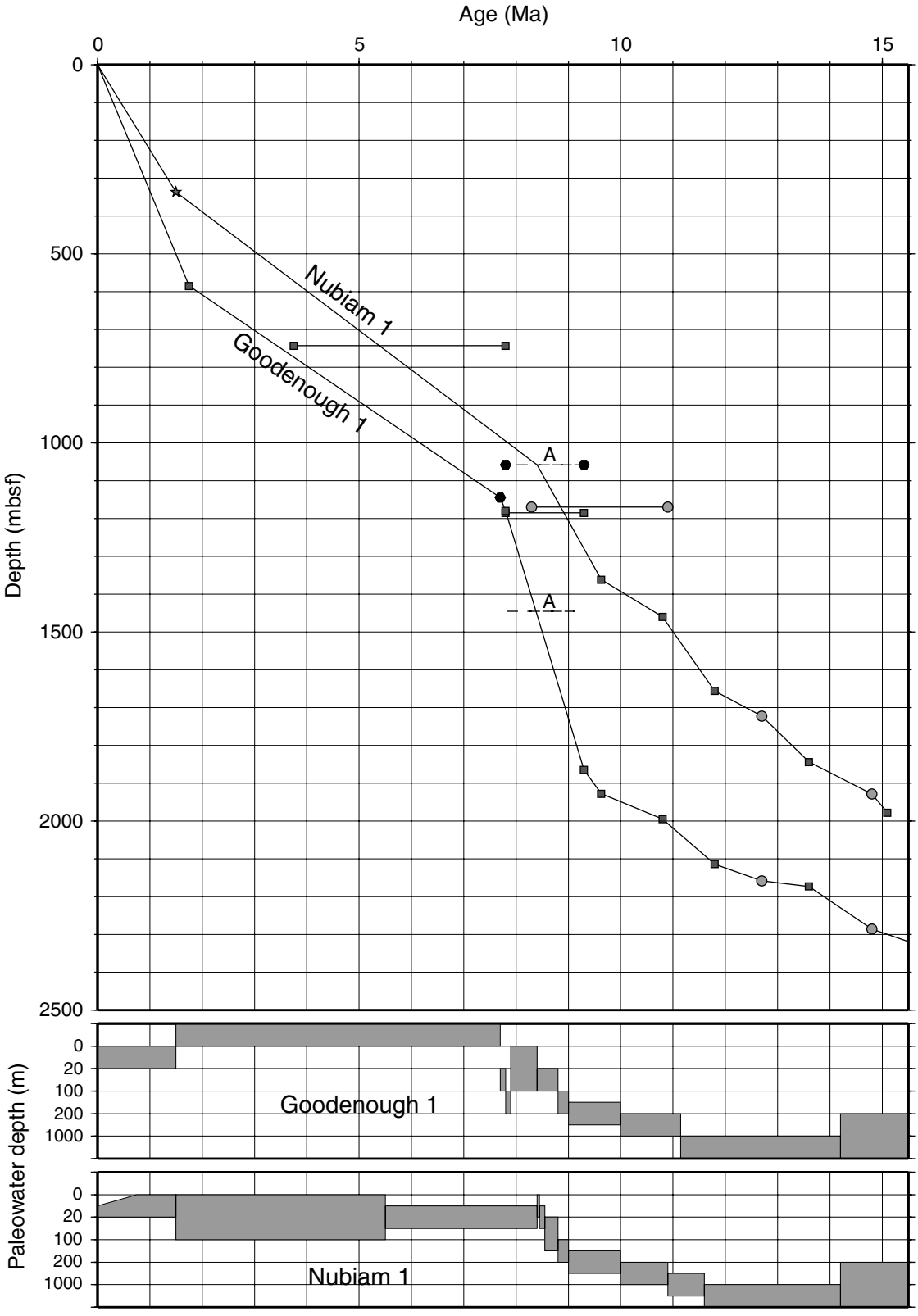

Figure F6. Lithostratigraphy and correlation of Leg 180 sites (Shipboard Scientific Party, 1999). Basement ages after **Monteleone et al.** (this volume).

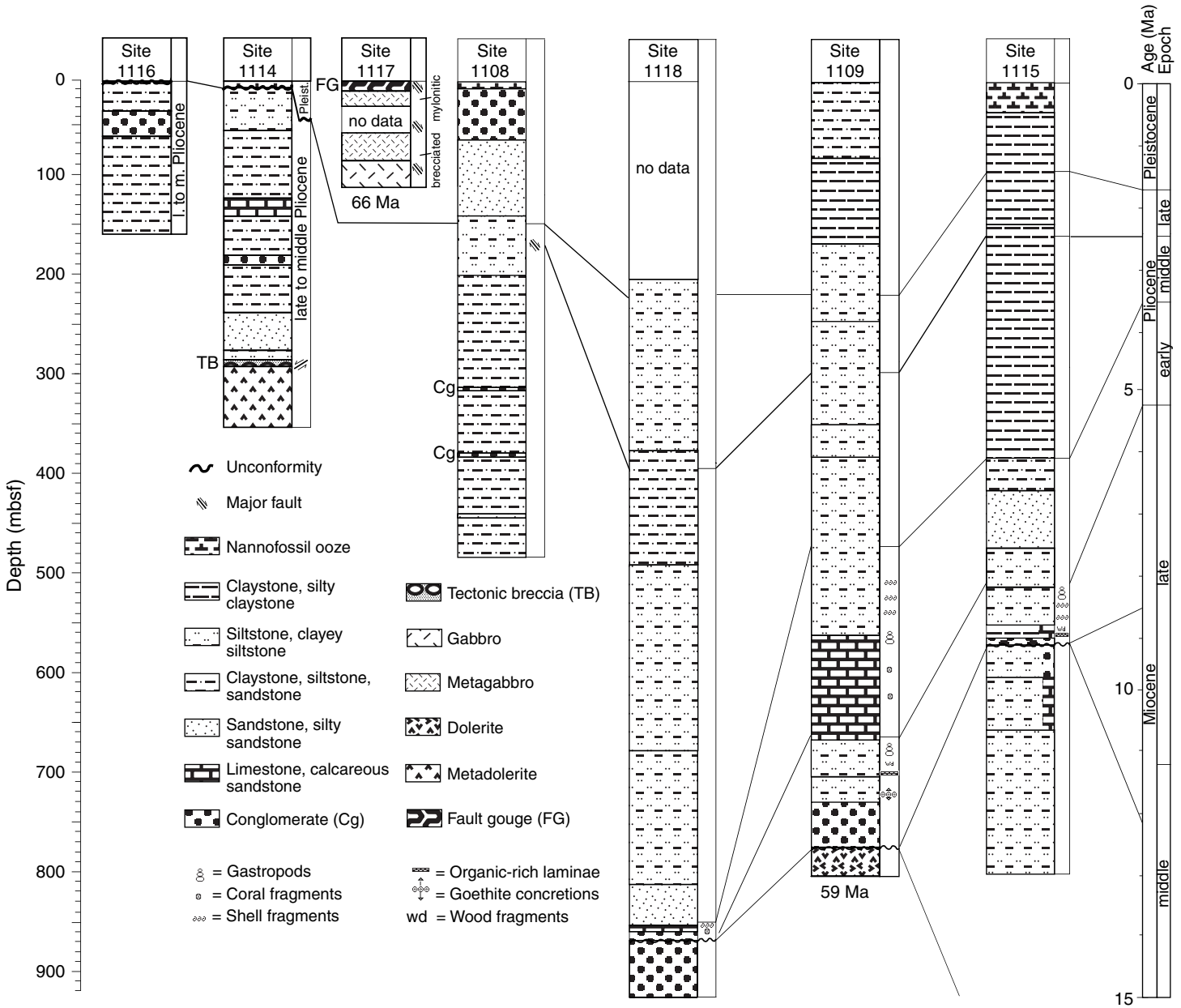

Figure F7. Sedimentation curves and paleobathymetry ranges for Leg 180 Sites, modified after **Takahashi et al.** (this volume). Wavy line indicates unconformity; other symbols as in Figure **F5,** p. 31.

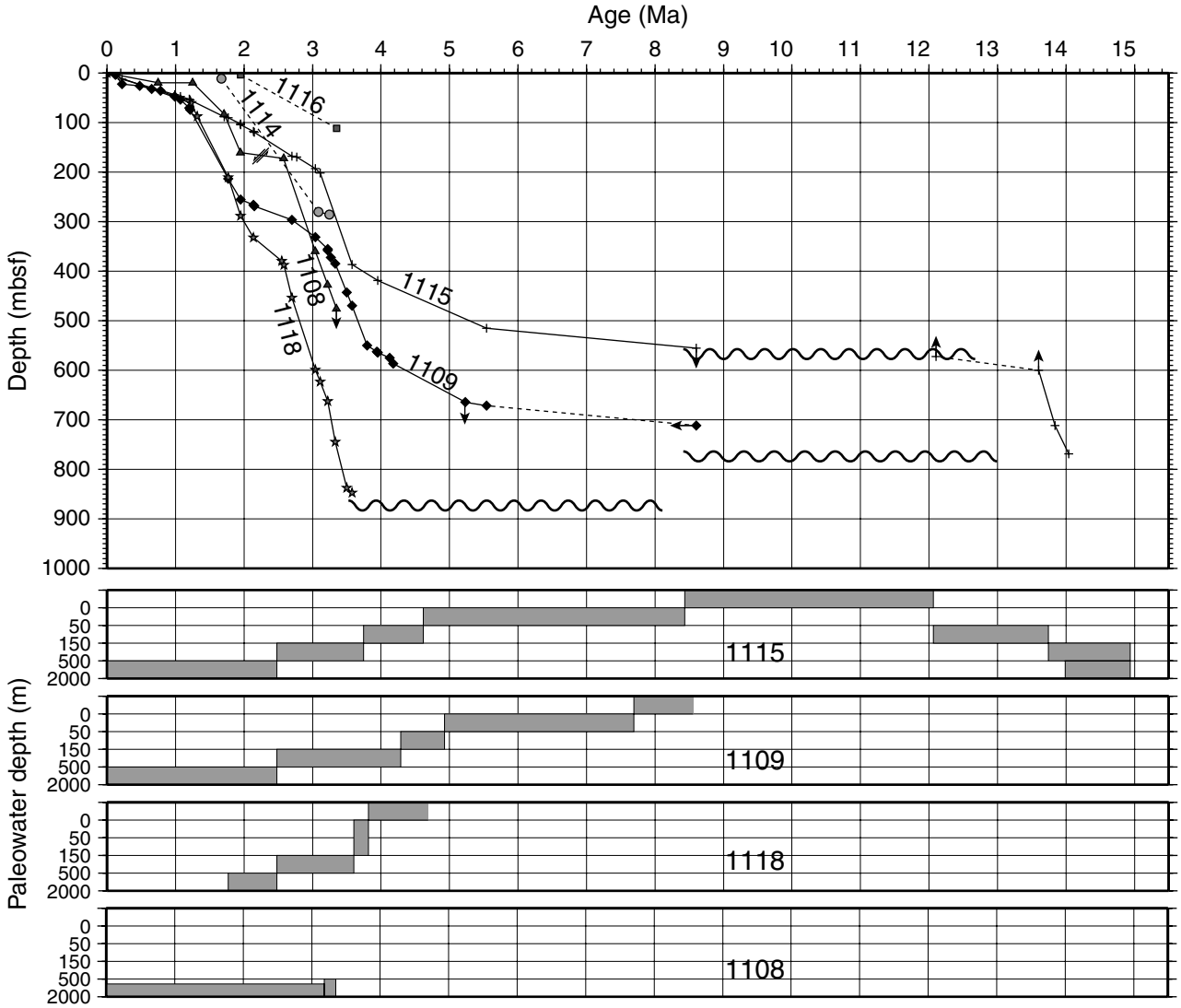

Figure F8. Interpreted line drawing of MCS profile 1366 (top panel), reconstructed at 1.6, 2.55, 3.2, 3.8, and 5.5 Ma (lower panels) using constraints from seismic stratigraphy (**Goodliffe et al.,** this volume) and paleowater depths (Fig. **F7,** p. 33) (Shipboard Scientific Party, 1999).

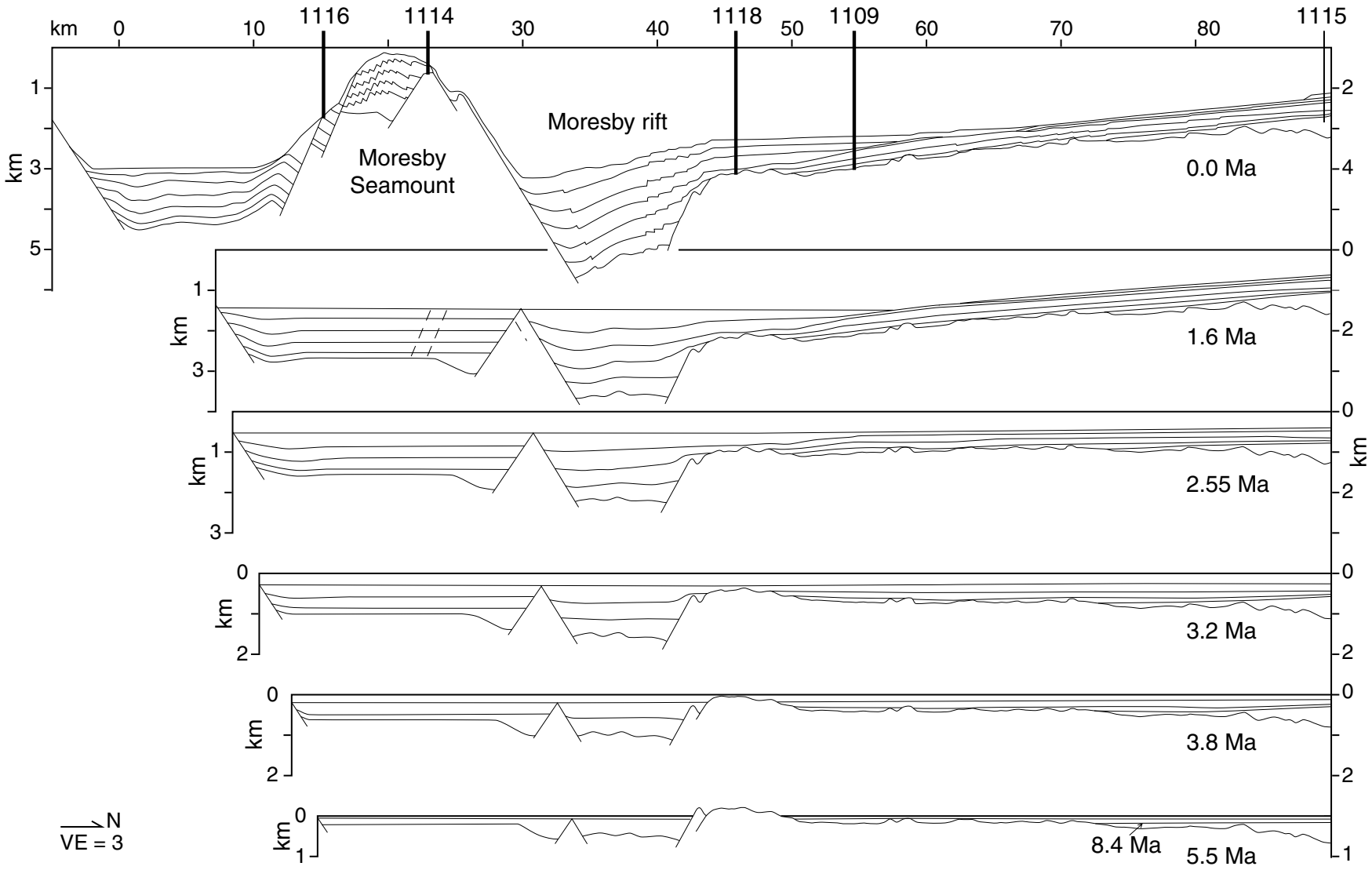

Figure F9. Biogeochemical profiles in sediments from the northern margin (Woodlark Rise) Sites, Leg 180 (Shipboard Scientific Party, 1999). **A.** Total bacterial populations at Sites 1109, 1115, and 1118. The solid curve represents a general regression line of bacterial numbers vs. depth in deep-sea sediments (Parkes et al., 1994), with 95% upper and lower prediction limits shown by dashed curves. **B–D.** Sulfate, ammonia, and methane depth profiles at Sites 1118, 1109, and 1115. The unconformity at each site is represented by the wavy line. **E.** C_1/C_2 ratios at Sites 1108, 1109, 1115, and 1118.

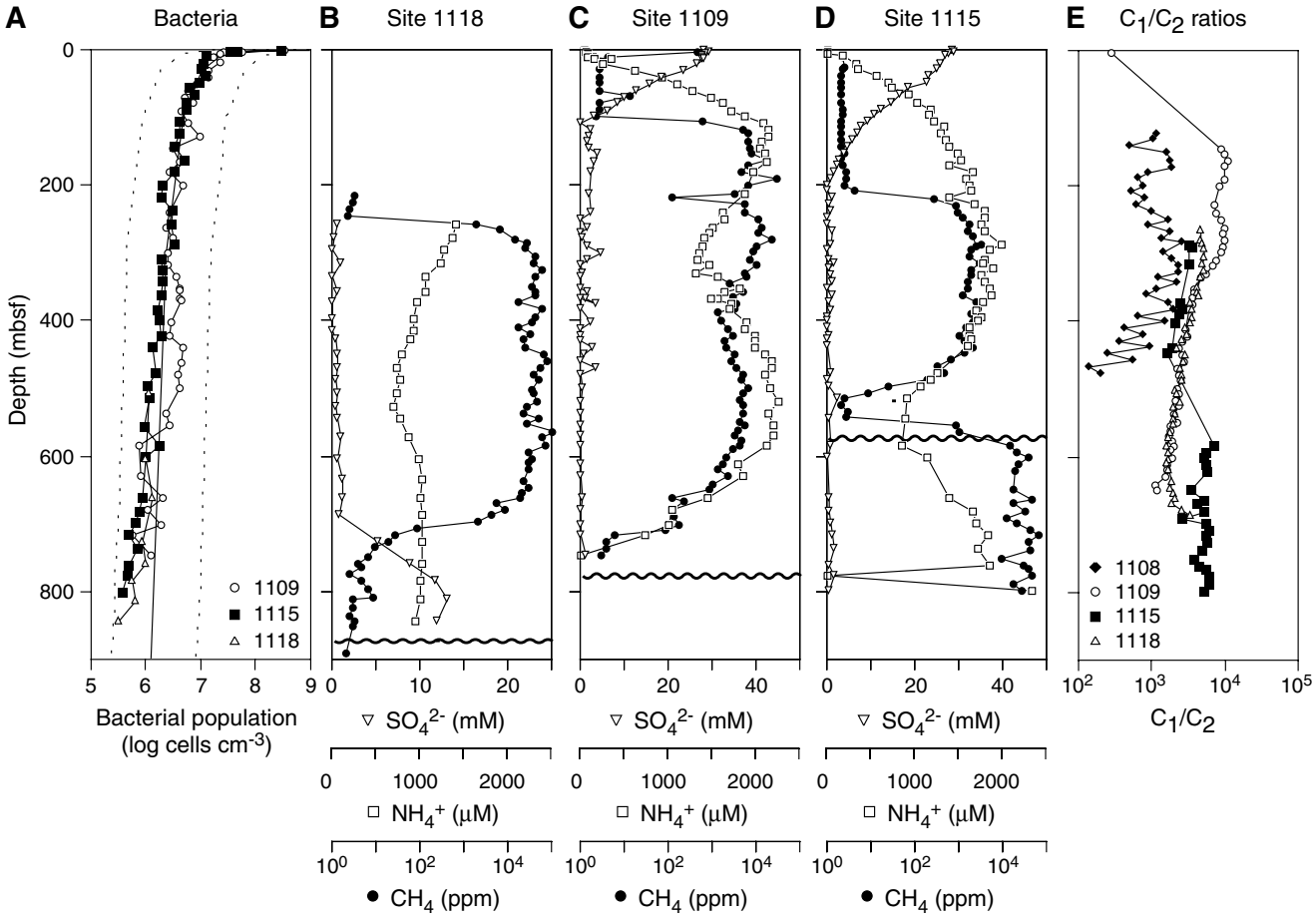

CHAPTER NOTE*

N1. Wellsbury, P., Mather, I., and Parkes, R.J., submitted. Geomicrobiology of low organic carbon sediments in the Woodlark Basin (ODP Leg 180): *FEMS Microbiology Ecology*.

*Dates reflect file corrections or revisions.